

**MORPHOLOGICAL INVESTIGATION OF AFR-PEPA-N IMIDE  
OLIGOMERS AND THEIR CURED POLYIMIDES  
AND THE REMODIFICATION OF AFR-PEPA-N TO ACHIEVE  
LIQUID-CRYSTALLINE BEHAVIOR**

A Thesis

by

LINDSAY ADAMS MURPHY

Submitted to the Office of Graduate Studies of  
Texas A&M University  
in partial fulfillment of the requirements for the degree of

MASTER OF SCIENCE

August 2003

Major Subject: Mechanical Engineering

**MORPHOLOGICAL INVESTIGATION OF AFR-PEPA-N IMIDE  
OLIGOMERS AND THEIR CURED POLYIMIDES  
AND THE REMODIFICATION OF AFR-PEPA-N TO ACHIEVE  
LIQUID-CRYSTALLINE BEHAVIOR**

A Thesis

by

LINDSAY ADAMS MURPHY

Submitted to the Office of Graduate Studies of  
Texas A&M University  
in partial fulfillment of the requirements for the degree of

MASTER OF SCIENCE

Approved as to style and content by:

---

Roger J. Morgan  
(Chair of Committee)

---

Terry Creasy  
(Member)

---

Dimitris Lagoudas  
(Member)

---

John Weese  
(Head of Department)

August 2003

Major Subject: Mechanical Engineering

## ABSTRACT

Morphological Investigation of AFR-PEPA-N Imide Oligomers  
and Their Cured Polyimides and the Remodification of AFR-PEPA-N  
to Achieve Liquid-Crystalline Behavior. (August 2003)

Lindsay Adams Murphy,

B.S., Texas A&M University

Chair of Advisory Committee: Dr. Roger J. Morgan

The morphological investigation of AFR-PEPA-N and the development of a new polyimide have been established herein. AFR-PEPA-N is an imide oligomer that was created out of the need to attain a high temperature polyimide that is also resistant to hygrothermal and thermooxidative degradation. Previously, AFR700B was implemented in aerospace applications, but it was found to be hygrothermally unstable. It experienced a severe drop in its glass transition temperature and composite blistering. AFR700B was improved upon, by altering the chemical structure of the polyimide. The nadic end-cap was removed and replaced by a more hydrolytically stable end-cap. However this phenylethynyl-terminated end-group could possibly create semi-crystallinity or liquid-crystalline characteristics within the polymer.

Previous research suggests further study of the relationships between AFR-PEPA-N's oligomer crystallinity and the properties of phenylethynyl-terminated polyimides. This understanding is valuable in processing AFR-PEPA-N by resin transfer molding (RTM) to obtain its optimum properties. The investigation included the

identification of a processing window, temperature overlap between the melting of residual crystals and crosslinking reactions, and liquid crystallinity behavior. These reactions were investigated primarily through birefringence.

The residual crystals were found to be innate in the oligomer powder and not created by preliminary thermal processing. Therefore a reasonable processing window was found based upon the reduction of crystal size by appropriate dissolution techniques. Possible nematic liquid-crystalline characteristics were found to be present at 360°C.

A new imide oligomer, which was based upon AFR-PEPA-N's original structure, was synthesized. The non-linear, fluorinated backbone of AFR-PEPA-N was replaced with a co-linear backbone, pyromellitic dianhydride (PMDA). These modifications were made in hopes to improve upon the network structure by it becoming more regular and resistance to nano-sized defects in the final crosslinked structure. The initial characterization found that the new polyimide, AFR-P3, displayed a cure temperature at 350°C. The degree of cure reaches about 80 to 90 percent complete based upon the consumption of the carbon-triple bond. AFR-P3 did not show signs of liquid-crystalline behavior. However, there will be future work in creating a more rigid-rod, self-assembling oligomer that can attain optimum thermal and mechanical properties.

## ACKNOWLEDGEMENTS

First of all, I would like to thank my advisor and mentor, Dr. Roger J. Morgan. His continuous efforts to be on the edge of cutting technology motivates me to do the best that I can and to stay on top of the latest developments in science and technology. His approach to polymer science and how he compares polymer phenomena to every day life is admirable and refreshing. His continuous guidance and support was so very valuable to me throughout this research. I have learned much from him, not only in academics but also how to mentor people. His loyalty to his students will leave a long-lasting impression on me. I am also very thankful and privileged to have Dr. Terry Creasy and Dr. Dimitris Lagoudas for serving on my thesis committee.

I am indebted to Steven Shanley and John Anthony, two very diligent undergraduate mechanical engineering students whose hard work and willingness to learn paved the way for this research. I am very grateful to the post-docs and graduate students in the Polymer Technology Center. If it was not for their invaluable advice and assistance in my times of need, the completion of this research would not be possible. I want to express my gratitude to Dr. Jim Lu, Yuntao Li, Jeff Boo, Ki Tak Gam, and Minhao Wong. They helped me become adjusted to working in the chemistry laboratory and taught me so much more than I could ever learn in a classroom. Also special thanks to Dr. Karaman and Mohammed Haouaoui for allowing me and my undergraduate research assistants to use their facilities.

I am very thankful to have worked with such wonderful graduate students from around the globe, whose cultures and lifestyles have added so much more richness to my own life. Thank you for sharing your lives with me.

I would also like to express thanks to Dr. Harry Hogan for encouraging me to go into graduate school and for creating a good first impression of what graduate school is truly like.

I am very grateful to my parents, Richard and Laurie Adams, for their willingness to provide an excellent education for me. They have educated me outside of the classroom by teaching me to be observant of the world around me and encouraged me not only in science and math but also in the visual arts. Because of their dedication, I received an excellent high school education. I have so much gratitude for my high school physics teachers, Mr. Loewer and Mr. Sload, who are by far the most exciting, unique teachers I have ever learned from. Their dedication to their students is incredible, and because of their efforts, I chose to major in mechanical engineering. I am so utterly thankful to my dear husband, Bryan. His unconditional love, support, and encouragement were so valuable to me. He gives me courage to face the hardships in my research. Finally, I would like to thank my Lord Jesus for giving us such a beautiful and intricate world to explore and the ability to comprehend it.

## TABLE OF CONTENTS

	Page
ABSTRACT .....	iii
ACKNOWLEDGEMENTS .....	v
TABLE OF CONTENTS .....	vii
LIST OF FIGURES.....	x
LIST OF TABLES .....	xii
CHAPTER	
I INTRODUCTION .....	1
1.1 Focus of Research .....	1
1.2 Background .....	1
1.3 Program Goals.....	6
II LITERATURE REVIEW .....	10
2.1 Introduction .....	10
2.2 History and Development of Polyimides .....	11
2.3 Polyimide Applications .....	12
2.4 Fundamentals of Polyimide Structure-Property Relationships .....	16
2.4.1 Polyimide Degradation and Stability .....	16
2.4.1.1 Effect of the Polyimide’s Dianhydride, Diamine, and End-group Structure on Stability .....	16
2.4.1.2 Thermal and Thermooxidative Degradation .....	19
2.4.1.3 Hygrothermal Degradation.....	20
2.4.2 Effect of Polyimide Structure on Crystallinity.....	22
2.4.3 Effect of Polyimide Structure on Solubility .....	24
2.5 Liquid-Crystalline Polymers and Their Properties.....	25
2.6 Previous Research .....	31
2.6.1 AFR700B .....	31
2.6.2 LaRC© PETI-5.....	34
2.6.3 AFR700C .....	37
2.6.4 Liquid-Crystalline and Rigid-Rod Polymers.....	41

III	MORPHOLOGICAL INVESTIGATION OF AFR-PEPA-N IMIDE OLIGOMERS AND THEIR CURED POLYIMIDES.....	45
3.1	Introduction.....	45
3.2	Experimental Techniques.....	49
3.2.1	AFR-PEPA-N Imide Oligomer Film.....	49
3.2.2	AFR-PEPA-N Melting and Curing Characterization.....	50
3.2.3	AFR-PEPA-N Ratio Film.....	51
3.2.4	Crystal Dissolution Characterization.....	51
3.2.5	Liquid Crystal Characterization.....	53
3.3	Results and Discussion.....	56
3.3.1	Crystal Structure and Morphology Results.....	56
3.3.1.1	Crystal Size as a Function of Imide and Temperature.....	56
3.3.1.2	Ratio-Morphology.....	61
3.3.2	Furnace Curing Results.....	62
3.3.3	Shear Test Results.....	66
3.3.4	X-Ray Results.....	67
3.3.5	Solubility Results.....	68
3.4	Conclusions.....	70
IV	REMODIFICATION OF AFR-PEPA-N TO ACHIEVE LIQUID-CRYSTALLINE BEHAVIOR.....	72
4.1	Introduction.....	72
4.2	Experimental Technique.....	75
4.2.1	Synthesis Preparation.....	75
4.2.2	Synthesis Procedure.....	76
4.2.3	Initial Characterization.....	79
4.2.3.1	Differential Scanning Calorimetry (DSC).....	79
4.2.3.2	Fourier Transform Infrared (FTIR).....	80
4.2.3.3	Dissolution and Liquid-Crystalline Test.....	81
4.3	Results and Discussion.....	81
4.3.1	Differential Scanning Calorimetry (DSC) Results.....	81
4.3.2	Fourier Transform Infrared (FTIR) Spectroscopy and Degree of Cure Results.....	83
4.3.3	Dissolution and Liquid-Crystalline Results.....	86
4.4	Conclusions.....	88
V	CONCLUSIONS.....	89
5.1	Conclusions.....	89
5.2	Suggestions for Future Work.....	90



REFERENCES .....	Page 91
APPENDIX .....	94
VITA .....	95

## LIST OF FIGURES

FIGURE	Page
1 AFR700B chemical structure, [3] .....	4
2 LaRC© PETI-5 chemical structure, [3] .....	4
3 AFR-PEPA-N imide oligomer chemical structure, [3] .....	5
4 Structure-Processing-Properties of AFR-PEPA-N Polyimide .....	7
5 Arrangement of molecules in liquid crystals (1 <sup>st</sup> row) and textures of liquid crystals in polarized light (2 <sup>nd</sup> row): (a) nematic, (b) cholesteric, (c) smectic, [10] .....	28
6 AFR700B chemical structure, [3] .....	31
7 LaRC© PETI-5 chemical structure, [3] .....	34
8 AFR-PEPA-N imide oligomer chemical structure, [3] .....	38
9 Synthesis of AFR-PEPA-N imide oligomers, [3] .....	39
10 Typical DSC trace of imide oligomer at heating rates of 20°C/min (AFR-PEPA-2), [3] .....	47
11 (a) Micrograph of AFR-PEPA-2 imide oligomer powder in NMP at room temperature, undissolved oligomer crystals. (b) Micrograph of AFR-PEPA-2 imide oligomer powder in NMP at room temperature, same crystals that are stressed and broken up.....	52
12 Shear experimental apparatus setup .....	54
13 AFR-PEPA-2 imide oligomer film morphology with average crystal length as a function of temperature, viewed at room temperature .....	57
14 AFR-PEPA-4 imide oligomer film morphology with average crystal size as a function of temperature, viewed at room temperature .....	58
15 AFR-PEPA-8 imide oligomer film morphology cast at different isotherms and viewed at room temperature.....	60

FIGURE	Page
16 50-50 Ratio of AFR-PEPA-4 and AFR-PEPA-8 .....	61
17 75% AFR-PEPA-8 combined with 25% AFR-PEPA-4 .....	61
18 AFR-PEPA-2 film morphology at varying isotherms held at fifteen minutes each, viewed at room temperature (a-f).....	64
19 Liquid-crystalline behavior at 360°C cure for both PEPA-2 and PEPA-4, viewed at room temperature .....	65
20 AFR-PEPA-2 film morphology result of manually applied shear, viewed at room temperature .....	66
21 Wide-angle x-ray diffraction plot of AFR-PEPA-2 film .....	67
22 AFR-PEPA-2 imide oligomer: 0.01g / 10 ml NMP blended for 24 hr. at 23°C .....	68
23 Morphology of self-assembled rigid-rod oligomers.....	72
24 Co-linear chemical structure exhibited by PMDA and <i>p</i> -PDA.....	75
25 Synthesis of TAMU-P3-N.....	78
26 DSC plot of TAMU-P3-1 from 23°C to 500°C at a rate of 20°C per minute.....	82
27 FTIR plot of TAMU-P3-1, uncured, showing significant imides and carbon-triple bond peak intensities.....	83
28 Degree of cure of TAMU-P3-1 at 340°C over time, comparing normalizing imides .....	86
29 Pictographs of undissolved TAMU-P3-1 imide oligomer crystals and heated to 360°C and held at 360°C for 10 minutes (seen in real time).....	87

## LIST OF TABLES

TABLE	Page
1 Chemical structure related to crystallinity, [4].....	23
2 Dissolution tests as a function of time and temperature.....	53
3 Crystal dimensions as a function of oligomer and processing temperature.....	59
4 Observed oligomer film morphology at different annealing temperatures.....	62
5 Peak assignments to normalize the intensity of the crosslink reaction.....	84

# CHAPTER I

## INTRODUCTION

### 1.1 Focus of Research

This research is part of the Advanced Research Project funded by the State of Texas, Materials Science ARP grant number 000512-0190-2001 through the TEES Institution of Texas A&M University. Dr. Roger J. Morgan served as the head of this investigative research and project. This project also collaborated with the Air Force Research Laboratory / Wright-Patterson Air Force Base.

### 1.2 Background

In the aerospace and automotive industries, there is a demand for high performance materials. The materials must possess a great strength to weight ratio yet fulfill the performance and processing criteria. Composites can usually meet the needs of the design, and are the ideal materials for aerospace applications due to their lightweight, high strengths, and radar transparency. The performance of the composites often relies on the properties of the polymer matrix. The polymer is a limiting factor together with the fiber-matrix interface in the composite due to the high thermal and

fatigue endurance of the carbon fibers. The composites are exposed to a range of extreme thermal gradients, hygrothermal and thermo-oxidative service environments, fatigue and high stresses. Polymers commonly implemented in aerospace composite matrices, are epoxies, polyimides, and bismaleimides [1, 2, 3].

Epoxies can be processed at relatively low thermal conditions, unfortunately they cannot be used in applications that experience high hygrothermal conditions. This is due to their high moisture intake that eventually leads to plasticization and weakening of the epoxy matrix [3].

It has been found that polyimides exhibit excellent thermal and mechanical properties for future aerospace applications. They have an overall mixed hydrolytic stability and good resistance to wear and radiation, and inertness to solvents [3, 4]. The first aromatic polyimide was synthesized in 1908, but it was not further developed until the late 1950's. Through the efforts of DuPont, polyimides were more fully developed and finally made commercially available in the early 1960's. Now many research groups have synthesized a variety of new polyimides with varying characteristics to meet the needs of specific designs and applications [3,4].

Polyimides are used as high-temperature adhesives, in microelectronics, optoelectronics, photoresists, nonlinear optical materials, aerospace applications, composites, and fiber optics. Polyimides are highly used in the optics and electronics

areas possibly due to their low dielectric constant and low relative permittivity [4]. But because of their high thermal capabilities, they can be somewhat troublesome to process at high temperatures and viscosity.

Also polyimides will hydrolytically degrade. This is when water molecules attack their imide ring, and the polyimide will experience a reverse imidization, and/or depolymerization. The polyimide will revert back to the polyamic acid. Chain scission of polyamic acid results in an acid monomer, which will increase the degradation of the polyimide [1,5]. The acid is 550 times more susceptible to hydrolysis than the imide ring [3]. This overall chemical degradation will decrease the polyimide's thermal capabilities, and overall adversely affect the mechanical properties of the composite.

Thermoset bismaleimides contain some desirable properties relative to polyimides and epoxies. That is, they are easier to process than polyimides, yet have a glass transition temperature that is comparable to polyimides. However, bismaleimides are very brittle and some have observed galvanic corrosion in the polymer when in conjunction with carbon fibers [3].

From the basis of PMR-15, AFR700B was created, by the Air Force, out of a need to have a polyimide perform similar to other polyimides, but can perform at a higher service temperature of 371°C. Its chemical structure is shown below in Figure 1. Despite AFR700B's excellent thermooxidative resistance, thermal capabilities, and

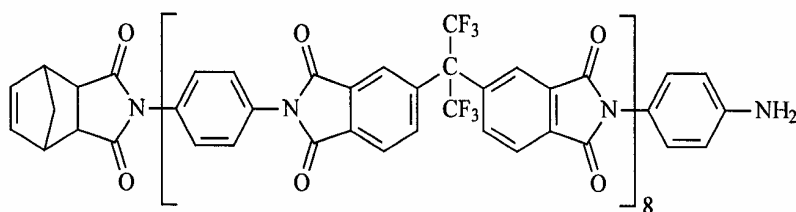


**Figure 1.** AFR700B chemical structure, [3].

mechanical performance, it did not perform well in a hygrothermal environment [3]. However, it was found that the norbornene crosslinks associated with the Michael addition model created the hydrolyzable weak link in AFR700B [1, 3]. Therefore, Lincoln concluded that the AFR700B polyimide must be end-capped with a much more hydrolytically stable functional group [3]. This hydrolytically stable group was found in PETI-5. PETI-5 is a thermoset phenylethynyl-terminated imide oligomer that drew much attention during the High Speed Civil Transport Program. The phenylethynyl oligomer end-caps are considered the ‘strong link’ in the PETI-5 chemical structure as seen in Figure 2.

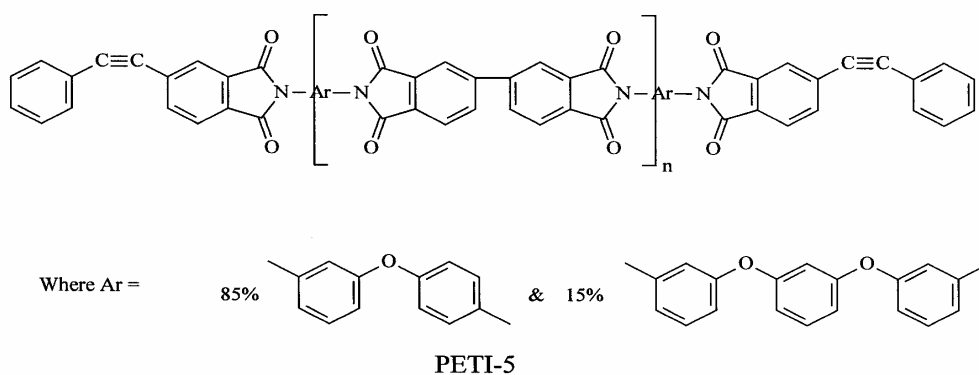


**Figure 2.** LaRC© PETI-5 chemical structure, [3].



The PETI-5 endcaps were incorporated into the AFR700B structure. AFR-PEPA-N was synthesized in hopes of combining the thermooxidative abilities of AFR700B with the hydrolytic stability of PETI-5 and is able to withstand prolonged temperatures equivalent to AFR700B. The new polyimide, shown in Figure 3, was

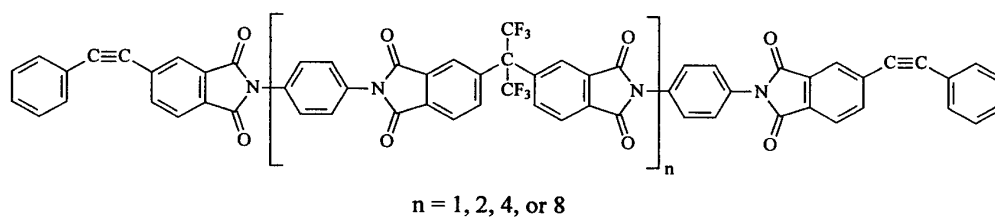


**Figure 3.** AFR-PEPA-N imide oligomer chemical structure, [3].

found to have superior hydrolytic stability similar to PETI-5 and has excellent mechanical properties at high temperatures. A correlation was found between the polyimide's mechanical response and its crystallinity, but this relationship was not well-understood [3].

### 1.3 Program Goals

The thesis will investigate any possible (i) crystalline and (ii) liquid-crystalline nature of the precured and cured polyimide oligomer, AFR-PEPA-N, as a function of chemical composition, temperature, molecular weight, and oligomer synthesis conditions, by birefringence. The results of this research will aid in optimizing the structure-property-processing relationships of polyimides for use in resin transfer molding (RTM) processing of complex shaped composites.

The thesis will specifically address several key items:

- ◆ Identification of a reasonable processing window.
- ◆ Residual oligomer crystals acting as stress concentrators and initiators of microcracking.
- ◆ A potential temperature overlap between the melting of crystals and the curing of the polyimide.
- ◆ Possible crystalline and/or liquid crystalline characteristics.
- ◆ Synthesis of new polyimide that has a higher potential for liquid-crystalline characteristics.

Figure 4 details the optimization of the structure- processing-properties in a graphic format.

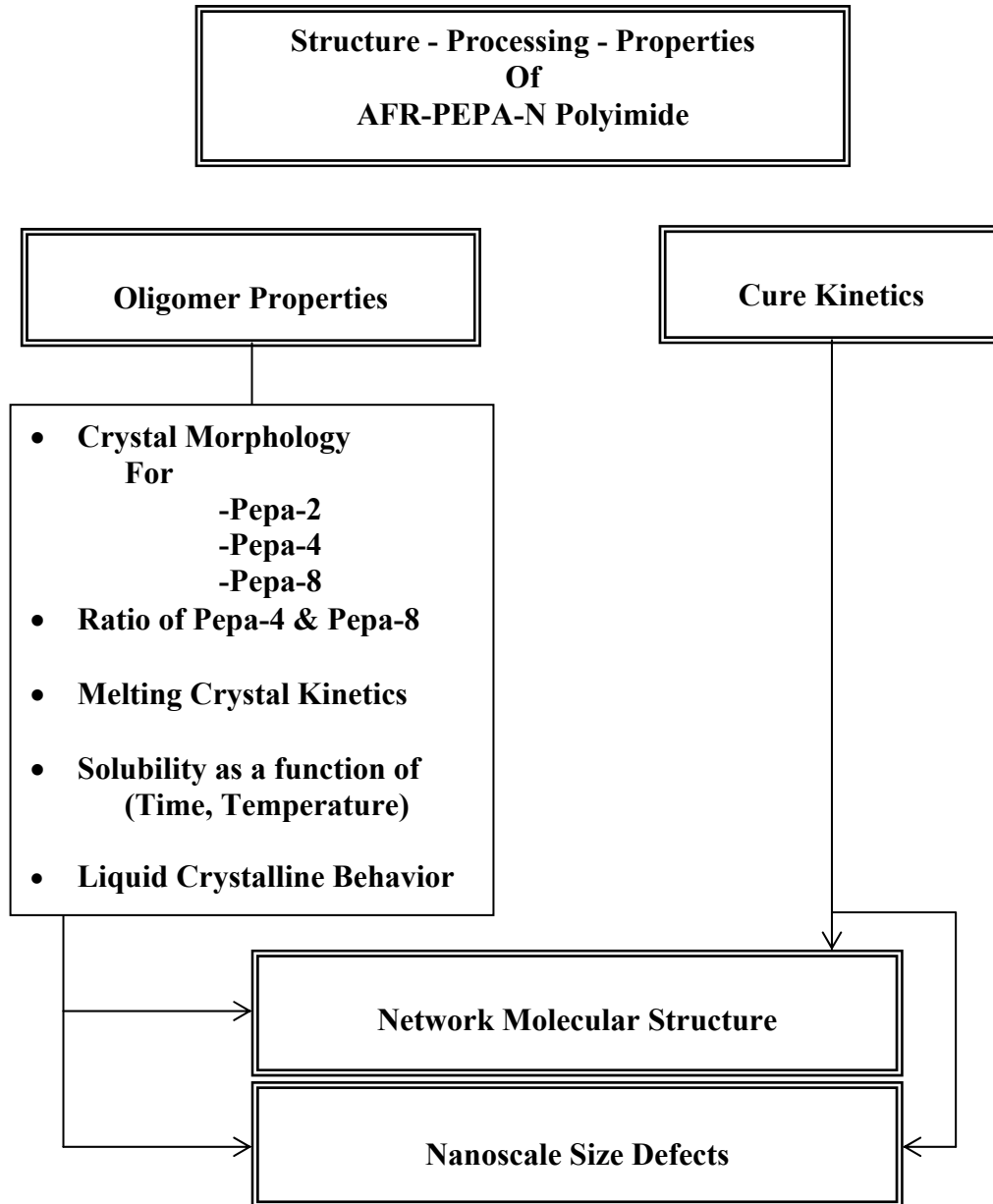


Figure 4: Structure - Processing - Properties of AFR-PEPA-N Polyimide

Based on the results and liquid-crystalline characteristics of AFR-PEPA-N, a new polyimide will be synthesized in an attempt to create a more rigid-rod molecular structure. The rigidity of the oligomer may determine its liquid-crystalline behavior. These modifications are made in hopes to improve upon the network structure and resistance to nano-sized defects in the final crosslinked structure. This network structure would be constructed by crosslinkable imide oligomers that self-assemble.

The morphological investigation of AFR-PEPA-N and the development of a new polyimide establish the scope of this Master's Thesis. The details of the morphological investigation contain the identification process of the processing window, residual crystals, and liquid crystallinity behavior. The tools needed to investigate these details are the polarizing optical microscope and the wide-angle x-ray (WAX) diffraction machine. Using these tools, the crystal morphology of the polyimide can be investigated over a spectrum of processing conditions.

This investigation of the morphology will contribute to the ability to process the material at reasonable time and temperature. It will also aid in processing a material with excellent mechanical properties, containing no nano-sized defects. This will aid in the research that has been developing polyimides, for RTM processing, that have superior mechanical and thermal properties [1, 6].

The synthesis of the polyimide, with the modified chemical structure, will further facilitate ongoing research for self-assembling nanorod macromolecules that “can be crosslinked to form films and fibers with superior thermal, mechanical, and photonic properties [7].”

## **CHAPTER II**

### **LITERATURE REVIEW**

#### **2.1 Introduction**

In this chapter, I will review the previous research concerning polyimides, liquid-crystalline behavior and rigid-rod polymers. In more detail terms, PETI-5, AFR700B and Aramid K3B research will be discussed and compared. The past research on rigid-rod polymers, especially polyimides, will be looked into, especially the structural requirements to achieve liquid-crystalline behavior. Also the synthesis of the new polymer, AFR700C, or AFR-PEPA-N, will be discussed and the critical factor that makes it different from AFR700B. The initial characterization of that polyimide will be discussed in further detail.

But before discussing the details of previous research, polyimide history, applications, and the fundamentals of polyimide degradation mechanisms will be presented.

## 2.2 History and Development of Polyimides

The first aromatic polyimide was synthesized in 1908, but it was not further developed until the mid-1950's. Through the efforts of DuPont, polyimides were more fully developed and finally made commercially available in the early 1960's [3,4]. During the early years, DuPont's Film Department focused upon creating a new product based upon 4,4'-dimethylheptamethylene diamine and pyromellitic dianhydride (PMDA). These efforts were to create a "convertible polymer" that could be changed easily and then converted to a permanent configuration. After much hardship, Andy Endrey helped make this "convertible polymer" a reality in 1956 [4]. The poly (amic acid) film was found to have great potential in the marketplace due to its excellent thermal, electrical, and mechanical properties.

After further development, the next step was to find potential applications and niche markets for placement of a polyimide resin. The Department of Defense, along with the electrical and aircraft industry, had a high level of interest in aromatic polyimide films. Large-scale processing of polyimides were researched by Yerkes Laboratory, in Buffalo, New York, and were able to propose an acceptable process for DuPont's facilities. In 1965, DuPont successfully created the first-ever polyimide film production line, which produced Kapton film [4].

From the initial research, many new polyimides were emerging. The National Aeronautics and Space Administration (NASA) had a high level of interest in the capabilities of polyimides. They conducted monumental research in this area, while creating and developing high-performing materials, such as “bis-maleimide composites, the LARC polyimide series, colorless polyimides, and poly (imide/etherketone) copolymers [4].” Due to the versatility and exceptional characteristics of polyimides, there are a wide variety of areas that polyimides can be applied to, such as electronics, high-performance composites, fibers and foams, coatings, adhesives, and film [4].

### **2.3 Polyimide Applications**

An advanced composite is a combination of an organic matrix and high-performance fibers or particles. These high-performance materials include carbon, boron, and Aramid materials that have advanced properties compared to the glass fiber commonly used in composite applications. The matrix limits the performance ability of the composite system.

The purpose of polyimides applied to advanced composites is due to the fact that polyimides are stable at high temperatures for long periods of time. The high thermal composite would be applied primarily to the aerospace industry, where military aircraft and missiles experience long-term high thermal environment [8]. Many polyimides have been developed primarily for the advanced composite applications, such as: LaRC-160,



PMR polyimides, PMR-II, Avimid K series, Avimid N, LaRC TPI, Polyetherimides (PEIs), and Polyamideimides [8].

Another important arena where polyimides are becoming popular is the semiconductor industry. Two main areas where polyimides are used are for protection or shielding and as an interlayer dielectric. Because of their ease of processability, good mechanical and thermal properties, and dielectric properties, polyimides offer much. They do have certain drawbacks compared to other materials used in the industry. They have a high moisture absorption and low thermal stability relative to other insulators. Polyimides can be used for a junction coat passivation, buffer coat, and alpha-ray shielding applications. The purpose of the junction coat passivation is to prevent the electrical device becoming contaminated. The buffer coats act as mechanical stress reliever and protect the components from excess moisture. The interlayer dielectric serves as insulation between wires. The alpha ray shielding is used for memory devices and protects against soft errors.

Photosensitive polyimides are very useful for processing in the semiconductor components. They are used as substrates between several layers of electrical devices. Photosensitive polyimides can be made to complex patterns using direct ultraviolet laser photablation, reactive ion etching (RIE), or scanning laser ablation (SLA) by a soft or hard mask, and wet etching [4]. The unexposed areas are removed during the

processing. Polyimide properties can be changed by their backbone. They can be covalent, ionic, or intrinsic types depending upon the backbone structure [4].

Polyimide material is most utilized in film form. The film is cast from polyamic acid solution and then is imidized by either thermal or chemical means. The films are one of the easiest to process and have very good properties. DuPont's Kapton® has been implemented in a number of applications such as aerospace cables and wiring, laminates, coatings for chips, capacitors, magnet wire, flexible circuits, transformers, and traction motors. Kapton's® glass transition temperature is 385°C and its resistance to solvents is very good [8]. Film orientation is also very important to the properties desired from the product. A film that is anisotropically oriented will have an increased tensile strength and modulus, and also absorb much less water.

Langmuir-Blodgett is a method that applies ultra-thin polyimide films in microelectronics. This technique allows for a single monolayer film with little to no defects that is formed on a water surface. The film is then transferred to a solid [4].

Gas Separation Membranes are another interesting use for polyimides. Polyimides were found to have an ability to selectively allow certain gases and vapors through its walls. Oxydianiline (ODA)-PMDA was found to have a high permeability to water vapor, oxygen and carbon dioxide. Further research found that the film could

allow a higher gas flow through and has a higher selectivity, by modifying the polyimide structure [8].

Polyimide foam is another area that has a large amount of applications due to polyimide's high thermal property, and mechanical strength due to the innate structural design that foams possess. Foams are especially valuable to the aerospace market where a great strength to weight ratio is highly prized. The foam could be used in walls, ceiling panels, as acoustical, vibration, and thermal insulation [8].

Some polyimides display properties that would make polyimides look like a very attractive material to use as a structural adhesive. Adhesives that can join many different materials (metals, ceramics, composites, and polymers) together in extreme environments are desired in many industries such as the aerospace, electronic, and automotive. Other requirements that the polyimide adhesive may need to fulfill could be temperature, thermal expansion limits, toughness, moisture absorption, fatigue limit, thermal gradients, chemical reactivity, and lifetime [8].

Adhesion to metal films is very important especially concerning polyimide use in the semiconductor industry. Typically there is a metal film that is sprayed upon a polyimide substrate. The interfacial adhesion between the two materials depends especially on the surface roughness of the polyimide, the chemical and environmental history of the polyimide, and how the metal is adhered to the polyimide [4].

## **2.4 Fundamentals of Polyimide Structure-Property Relationships**

### **2.4.1 Polyimide Degradation and Stability**

The purpose of reviewing the degradation of polyimides is to give purpose to the reasons for continuing the research and to layout a foundation before discussing the previous research on which this knowledge is based upon. The forms of degradation are important to understand when applying polyimide matrix composites as key structural members in an aerospace application. It is important to choose the proper polyimide based upon the requirements for the desired purpose.

#### *2.4.1.1 Effect of the Polyimide's Dianhydride, Diamine, and End-group Structure on Stability*

The stability of the polyimide is greatly dependent upon its chemical structure. It is not just the bonding energies that determine the ability to resist degradation but much more complicated system of mechanisms that are involved. These may be the chain packing, density, molecular weight, conformation, and location of functional groups.

These characteristics can control the opportunity of degradation initiation and the rate of degradation of the polyimide [4].

The types of diamines, dianhydrides, and end-groups may determine how the polyimide will degrade at a certain rate. Researchers have attempted to rank dianhydrides, diamines, end-group structures based upon the trends from many of the degradation studies. One common observation was that the dianhydride does not necessarily have much of an effect upon the stability of the polyimide [4].

However the diamine structure can be more of an influence upon polyimide stability than the dianhydride. Because the diamine has a higher electron density compared to the rest of the structure, the diamine can be the 'weakest' link. The high electron density acts as a magnet for an oxidation initiation point. Polyimides based upon electron deficient diamines tend to be more stable compared to others. Also the amount of fused rings in the diamine effected the stability of the polyimides. The greater the amount of rings the higher the probability of instability [4].

Another observation was that diamines containing an ether linkage were very stable and flexible. Flexibility allows for good solubility and polymer melt flow characteristics. These two characteristics make for better processing, and when the polyimide can be processed with out flaws the resistance to degradation will be very great [4].

Reactive end-groups are a very good way of increasing the stability of the polyimide. If the polyimide chains are not terminated, the chains will have either an amine or an anhydride at the end of each chain. Unfortunately these types of end-groups can be highly reactive with surrounding conditions that can decrease the polyimide's stability. A chain ending with an anhydride can cause hydrolytic degradation.

It was also observed that a chain ending with an amine group can be considerably more detrimental than a chain ended with an anhydride. The stoichiometry is very important when synthesizing a polyimide. It is better to have a slightly higher amount of dianhydride relative to the amount of diamine [4], [8].

The best way to avoid chain degradation is to add reactive end-groups to both ends of the polyimide chains. End-groups can limit the molecular weight of the polyimide. Limiting the molecular weight decreases the viscosities, which aids in the processing capabilities and melt stability of the polyimide. It also improves upon the thermal and oxidative stability. Several reactive end-caps that are implemented are maleimide, nadimines, acetylenes, and biphenylenes [4]. It was found that acetylene and biphenylenes offer higher thermal and oxidative stability relative to the malic and nadic anhydrides.

Acetylene-terminated polyimides can crosslink by the carbon triple bond via trimerization. This creates an aromatic ring that is assumed to be where the excellent thermal properties come from. The trimerization process does not undergo full crosslinking especially at the glass transition temperature. This can create a large difference in the properties of acetylene-terminated polyimide [4].

#### *2.4.1.2 Thermal and Thermooxidative Degradation*

Even though polyimides are the most thermally stable polymer, they can still degrade if the conditions are just so. They can degrade if exposed to high temperature for a very long period of time. This exposure can lead to physical and chemical aging and dramatically effect the thermooxidative stability of the polyimide. Being exposed to high temperatures over a long period of time can increase the polyimide's density and brittleness. Polyimides are also susceptible to chemical aging. The chemical structure can be modified due to the highly reactive environment the polyimide may be in. Excessive crosslinking and chain scission is just a few of the reactions that take place during chemical aging [3].

The polyimide's imide ring is possibly an initiator site for this degradation to begin. Typically there is a release of CO, CO<sub>2</sub>, and water from these bonding sites, when heated at high temperatures. Thermooxidation is one major form of chemical

aging [3]. Lincoln summarizes thermooxidation degradation mechanisms for polyimides in composite form at the macroscopic level in further detail, which is in the Appendix.

Not only does thermooxidation take place on the microscopic and macroscopic scale, but also on the molecular scale. Polyimides perform better if their dianhydride and diamine are at high oxidation states. This increases the resistance to thermooxidation degradation. 3,3',4,4'-benzophenonetetracarboxylic dianhydride (BTDA), oxydiphthalic anhydride (ODPA), PMDA, and 6F are several dianhydrides that are in high oxidation states. The thermooxidative stability changes for every diamine. It is found that biphenyl diamine units have the best overall thermooxidative stability. Benzophenone and *p*- or *m*-phenylene groups also follow. It has also been observed that high molecular weight polyimides have better thermooxidative resistance than lower molecular weight counterpart [8].

And as mentioned in the previous section, the use of reactive end-caps can greatly improve upon the thermal and thermooxidative resistance of the polyimide. Acetylene terminated polyimides have outstanding thermal properties [3], [8].

#### *2.4.1.3 Hygrothermal Degradation*

It is known that most polyimides can tolerate high thermal conditions, however these materials can degrade rapidly in an hygrothermal environment. This section will



cover what goes on during the hygrothermal environment to cause such degradation, and what results from the degradation. In general a hygrothermal environment is a combination of moisture and high temperature conditions. Lincoln lists the number of ways this degradation can occur by “moisture induced microcrack formation, hydrolytic degradation, molecularly ‘locked-in’ water, blister formation and subsequent composite delamination, and a variety of mechanisms resulting from hydrolysis and galvanic attack [3].”

Due to the high thermal integrity of the polyimide, it seems that the moisture content (in the surrounding environment and within the material itself) is the culprit for the polyimide degradation. One particular problem that polyimides suffer is that of hydrolysis and subsequent depolymerization. Polyimides chemically degrade when exposed to water. The amount of degradation due to hydrolysis greatly depends upon the chemical structure, diffusivity properties, and how the polyimide was processed. Hydrolytic attack can occur at the imide ring. Here the ring will open to an amide formation and that will lead to chain scission of the amide group [3].

#### 2.4.2 Effect of Polyimide Structure on Crystallinity

Polyimides have been observed to exhibit crystallinity in many instances. X-ray diffraction, FTIR, and optical methods have been used to observe the semi-crystalline morphology. Understanding the crystalline morphology of polyimides is important because the necessary properties of the polymer are directly influenced by the morphology [4, 8].

The backbone of the polyimide may influence the crystalline morphology. Researchers found that significant levels of crystallinity were found with some backbones and not so with other backbones, while using the same amine groups. Table 1 shows a brief list of combinations of different backbones and amine groups, along with their physical characteristics, that affect the polyimide's crystal morphology. Biphenyl dianhydride (BPDA) and OPDA did not have very significant levels of crystallinity. However, BTDA and PMDA backbones created a high amount of crystallinity in the polyimide [8]. The more linear and stiff the polyimide backbone is, there will be a higher amount of chain orientation within the material [4].

*Table 1. Chemical structure related to crystallinity [4].*

Polyimide Name	Physical Structure	Crystalline / Amorphous Results
BPDA/PPD	Stiff/Rigid	Semi-crystalline
PMDA/ODA	Rigid/Flexible	Semi-crystalline
BPDA/ODA	Stiff/Flexible	Semi-crystalline
BTDA/PPD	Flexible/Rigid	Semi-crystalline
BTDA/ODA	Flexible/Flexible	Amorphous
ODPA/ODA	Flexible/Flexible	Amorphous

X-ray diffraction studies found that polyimides exhibit peaks in the (00L) domain. However, this result can only be found in transmission, but not in the reflective mode. This is due to the high amount of alignment in the molecular chains that are in the film's plane. The lack of detail can create confusion to the crystalline system of the polyimide material [4].

### 2.4.3 Effect of Polyimide Structure on Solubility

When crystallinity develops in a polyimide, the solubility of the polyimide will decrease. It has been hypothesized that crystals act as physical crosslink sites, which inhibit dissolution [8]. This has been observed when partially imidized polyimides swell, but do not dissolve, when exposed to an organic solvent. It has also been suggested that partially imidized polyimides may contain premature crosslinks. These crosslinks would disappear after further imidization [4].

Solubility also depends upon the physical chemical structure of the polyimide. In general, the polyimides that are found to be quite soluble have very flexible chains. Three requirements or items that would give a polyimide a higher possibility of being soluble is that the backbone structure should contain polar groups. Bulky pendant or bridging groups and a higher flexibility allow for an improvement in solubility. The type of catenation of the polyimide is also important. Ortho catenation gives a polyimide a better solubility relative to meta catenation. 2,4'-catenation in a two-ringed diamine was able to improve the solubility in PMDA [4].

## **2.5 Liquid-Crystalline Polymers and Their Properties**

There has been a high level of interest in liquid-crystalline polymers (LCP) especially in the last two decades. Liquid-crystalline behavior was first discovered by Reinitzer in 1901, and was researched primarily in France and Germany for the next three decades [9]. It was not until the early 1980's when liquid-crystalline polymers were commercialized. It has been suggested that LCP's extraordinary properties open up a new realm of materials that can have superior properties relative to engineering thermoplastics. This is due to the ordering of the molecular backbones, oriented in a particular direction. This anisotropy produces exceptional mechanical, optical and electrical properties. Thermosetting LCPs can have a highly ordered; crosslinked matrix that creates an anisotropic material that could potentially perform in high stress and thermal environment [9].

There are two types of low molecular mass liquid crystallinity (LMMLC). They are thermotropic and lyotropic behavior. These types are divided by how the liquid crystal phase comes into being. The thermotropic behavior is that material transforms into the liquid crystal phase via a thermal process, whereas the lyotropic liquid crystals form by a solvent influence [9].

There is also another categorical way in which liquid crystals are divided. These three categories are based upon the ordering of the individual molecules, which are named: nematic, smectic, and cholesteric [9, 10]. Nematic is where the molecular centers are aligned in one particular direction. However this is only found in the microscopic volume, on the macroscopic level, the arrangement becomes much more disordered, because the intermolecular forces are quite small [9].

The cholesteric phase is similar to that of the nematic phase. However the phase is rotated about a single axis which is normal to the orientation of the molecules. This creates a helical path. The smectic phase is much more complex. The ordered molecules are layered upon each other, where each layer is a certain distance away from one another [9]. These three arrangements of liquid crystals are shown in the first row of Figure 5 [10].

The smectic phase can be separated even further into three conditions. Smectic A is similar to nematic, but the molecules tend to be more linear in direction, but be the least ordered compared to Smectic B and C. Smectic C's molecules are aligned and tilted at a particular angle. Smectic B has the highest amount of ordering, where the ordering takes place in two dimensions, rather than in just one [9].

The most common molecular shapes that create these types of phases are rods, discs, and lath-like molecules. Typically rods and discs are the most common geometric

forms that create liquid-crystalline behavior. Rods are found in all three types of phases. They have also created a cubic mesophase, however the reason for this behavior is unknown. The disc geometrical forms pack one on top of the other creating column-like structures. These columns will be found in a two-dimensional array, termed a columnar mesophase. These will orient in different geometrical forms having certain types of symmetries. Discs will also form nematic and smectic phases. Lath-like molecules create nematic phases where there is little rotation around the long axis of the molecule [9].

There are two basic types of LCPs. There can be main-chain or side-chain LCPs. The main difference between the two is how the mesogens are attached to the polymer backbone. There can also be combinations of the two designated types such as combined side-chain and main-chain LCPs. There are also LC elastomers and LC networks [9].

The optical microscope is an excellent tool in understanding the LC properties of a material. The polarizing optical microscope can be implemented to observe the liquid-crystalline “textures” of a thin layer of LC. These textures originate from the characteristic defects. These textures are unique and are a valuable tool in identifying the type of LC phase [10].

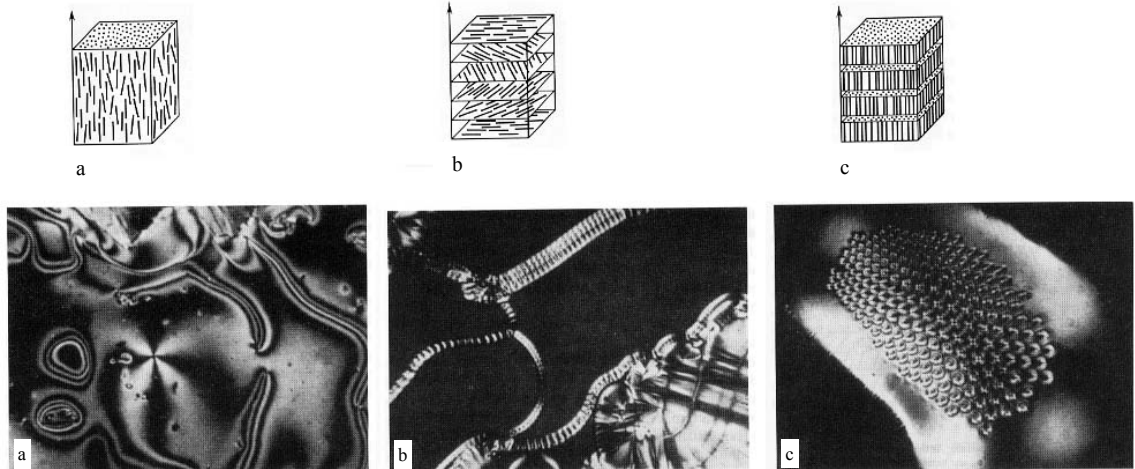


**Figure 5.** Arrangement of molecules in liquid crystals (1<sup>st</sup> row) and textures of liquid crystals in polarized light (2<sup>nd</sup> row). (a) nematic, (b) cholesteric, (c) smectic. [10]

The textures differ between the three types of packing patterns for liquid crystals, (a) nematic (b) cholesteric and (c) smectic. These unique textures show up very differently under the polarizing optical microscope, which are shown in Figure 5 [10].

These textures are given specific names and are modeled based upon the molecular configurations. There are four main textures observed in the nematic phase, which are the homogeneous (monodomain), Schlieren, Nematic droplet, and the Inversion wall [9]. There are other types of textures observed in the nematic liquid crystals such as a string-like texture and a marbled look.



The homogeneous texture has no specific texture observed in the microscope. Typically there is a homogeneous color observed. The monodomain texture can be viewed by “rubbing” the LC substrate along a glass surface [9]. The rubbing can be executed by placing the substrate in between two glass slides. The slides can be rotated and the phase becomes optically active due to the rotation about the molecules’ axes [10].

The Schlieren texture, which is shown in Figure 2(a), is the most observed texture in nematic LCs. The nuclei (dark points) are characteristic to the texture. There are large brushstrokes originating from these nuclei. The points are actually vertical defect lines that are termed disclinations. Depending upon the orientation of the disclinations and the molecular axes, the polarizer can be rotated and the position of the bands will move relative to the angle of the polarizer [9, 10].

There is also a special type of Schlieren texture. Typically when a glass substrate is rubbed a very straight band will be noticed in the polarizing microscope. This texture is known as the inversion wall. The molecules are aligned parallel to glass surface, but will not be straight at any walls. This texture is created mostly due to the activity between the layer and the encompassing walls [9].

The Nematic Droplet is another type of figure seen in the polarizing microscope that is only found in the nematic phase. The droplets form when the melt cools and begins to separate. It separates into an isotropic and nematic phases. The droplets are of the nematic phase and are completely surrounded by the isotropic phase. The molecular orientation in each drop can be different from one another. There are two types of orientations: bipolar and radial. As their names suggest, the molecules in the radial configuration are fanned out from the center of the droplet. The bipolar molecules are parallel to the surface wall of the droplet [9].

## 2.6 Previous Research

### 2.6.1 AFR700B

AFR700B was created, by the Air Force, out of a need to have a polyimide perform like similar polyimides, such as PMR-15, yet at an elevated service temperature of 371°C. PMR-15's backbone structure was changed from BTDE to 6FDA to improve the thermal stability. The diamine was changed to a *p*-PDA to decrease the toxicity levels. Only one end of the chain was capped with NE, with an amine on the other end of the chain as seen in Figure 6[3].

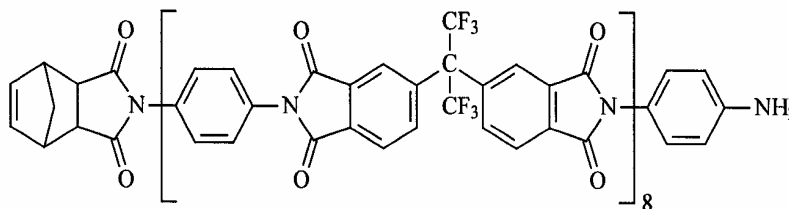


**Figure 6.** AFR700B chemical structure, [3].

The results of these changes were very successful. AFR700B had a glass transition temperature greater than 400°C. Compared to other polymer matrices, it had an additional heat tolerance of 150°C. Because of the great success, AFR700B was used immediately on the fuselage trailing edges on the F-117A Stealth Fighter [3].

Unfortunately AFR700B was found not to perform well in a hygrothermal environment, although it had an excellent thermooxidative resistance. The polyimide experienced a significant amount of hydrolysis, which lead to a large drop in  $T_g$  and mechanical properties. It has been postulated that this hydrolysis occurs at the crosslink, creating scission along critical intersection points. When the intersection is broken, the segments can not support the applied load. These scissions can create a major difficulty in the performance of the polyimide [3].

Lincoln researched how Avimid K3B and AFR700B hydrolytically degrade in pressure bomb experiments. Although AFR700B had excellent mechanical and thermal properties, it exhibited the worst overall hydrolytic degradation. Its glass transition temperature experienced a decrease of 25 to 200°C in an hygrothermal environment. The changes are due to hydrolytic degradation and plasticization via the entrapment of water molecules.

Blistering, a degradation mechanism was also found in the K3B and AFR700B specimens during the pressure bomb test. Blistering is controlled by several different variables such as (i) specimen geometry, (ii) high thermal gradients due to a high amount of heat over a short amount of time, and (iii) thermal-humidity-time history and the amount of contained moisture. Blistering eventually leads to delamination of the polyimide composite systems. After the pressure bomb tests, AFR700B experienced a dramatic change in dimensions, and several blisters were observed in its matrix. It was

found that only a small amount of moisture, in the AFR700B specimens, was needed to begin the blistering process. Only 0.4-wt.% moisture content was required to initiate blister formation [3].

Lincoln examined several different types of model compounds that make up the AFR700B system to understand what makes AFR700B hydrolytically unstable. The main crosslinking occurs within the norbornene and maleimide reactions. The norbornene reaction is made up of biradical homopolymerization and retro Diels-Alder reactions. But as the retro Diels-Alder experiences a temperature above 200°C it will release a cyclopentadiene [3]. If there is little to no pressure placed upon the polyimide, the norbornene crosslinking will create a high amount of Michael addition reaction products. The maleimide model groups contain the Michael addition reaction, aminolysis reaction, and the bismaleimide homocrosslink. Nadimide crosslinks, maleimide homocrosslinks, and the fluorinated backbone were all found to be hydrolytically stable.

However, it was found that the norbornene crosslinks associated with the Michael addition model created the hydrolyzable weak link in AFR700B [1, 3]. These norbornene crosslinks originate from the nadic end-caps. Therefore, Lincoln concluded that the AFR700B polyimide must be end-capped with a much more hydrolytically stable functional group [3].

## 2.6.2 LaRC® PETI-5

The PETI-5 is a thermoset phenylethynyl-terminated imide oligomer that drew much attention during the High Speed Civil Transport Program. It has been found to have excellent mechanical strength and toughness with a glass transition temperature at 270°C. It crosslinks between 320°C to 371°C range and at a pressure of 1 MPa and can be easily processed by resin transfer molding (RTM) [11].

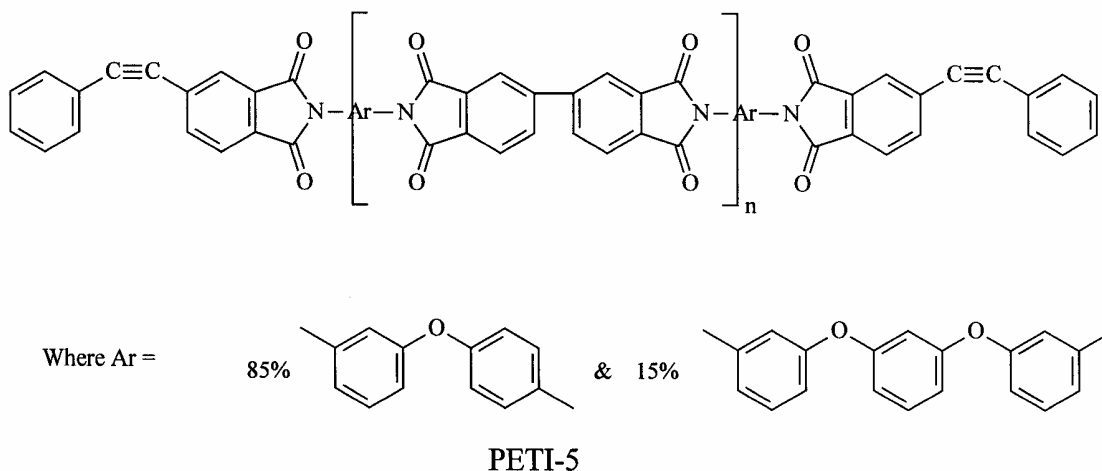


**Figure 7.** LaRC® PETI-5 chemical structure, [3].

In a comparative hygrothermal aging study with AFR700B and K3B, Lincoln concluded that PETI-5 was the most hydrolytically stable polymer. He also found that

there was  $10^{13}$  magnitude difference on the rates of degradation between AFR700B and PETI-5 [3]. This may be due to the phenylethynyl end-cappers.

The phenylethynyl oligomer end-caps are thought to be the ‘strong link’ in the PETI-5 chemical structure, as seen in Figure 7. It crosslinks via a carbon-triple bond mechanism within its phenylethynyl oligomer end-caps [11]. Acetylene-terminated polyimides were thought to cure via acetylene trimerization, yet later the curing kinetics was found to be much more complex [11]. The trimerization produces an aromatic ring at the crosslink site. This aromatic ring gives the polyimide the tolerance to high temperatures, stresses, and hygrothermal environments. Unfortunately the acetylene group only experiences 30% of the trimerization curing reaction and does not perform well when it nears its glass transition temperature [3, 8].

The PETI-5 network structure contains a high degree of chain extension and a low degree of crosslinking [5]. The high amount of chain extension gives PETI-5 an excellent toughness. PETI-5 can be either amorphous or semi-crystalline morphology due to how it is processed. It has also been found that PETI-5 will crystallize if the cure temperature is insufficient (350 + 360°C cure). The exact mechanism for this crystallization is unknown, but the reason for the semi-crystalline morphology is that crystallization inhibits crosslinking at this temperature range [3], [11]. Similar crystallization behavior has been observed in other phenylethynyl-terminated polyimides with different backbone structures [7].

The processing and curing mechanisms are complex and vary under different conditions. A semi-crystalline, partially crosslinked morphology is formed when cured at or below 350°C. The reason for this occurrence is that material consists of amorphous and crystalline phases. This system makes the processing of PETI-5 more complicated in that the crosslinking inhibits the growth of crystals.

Also it has been hypothesized that crosslinks and crystals both form by the phenylethynyl oligomer end-caps. When cured at 371°C, the material is completely amorphous [11]. At this temperature, the crosslinking kinetics of the system overpowers the crystal nucleation rate therefore giving rise to an amorphous polymer [3].

Lambert et. al. [3] suggests that crosslinking and crystallization in phenylethynyl-terminated polyimides is connected by three ways.

- “(i) Crosslinking eliminates reptation in its conventional sense, and only ‘reptation slack’ is available for movement along the polymer chains exceeding nanometers.
- (ii) The need for exclusion of the bulky crosslinks for crystallization to occur significantly reduces the rate of secondary nucleation, which results in a growth rate that decreases exponentially with crosslink density.
- (iii) The concentration of crosslinks controls the upper limit possible for lamellar thickness [3].”



Lincoln also concludes that there is a solubility limit upon how many crosslinks can exist in a crystal. This is based upon that if “the molecular weight between crosslinks is high, then the crosslinks can be incorporated into the crystals [3].” The opportunity for the polyimide to crystallize decreases when its crosslink density is too high.

The presence of the crystals gives a 10% increase in the materials mechanical toughness. Also the presence of crystals leads to a 170% decrease in ductility, relative to the amorphous material [11]. The crystals also create a higher concentration of defect sites cause a decrease in the strain to failure rate [3]. It was determined that PETI-5 has these properties due to the unique properties of the end-caps [11]. Replacing AFR700B’s hydrolytically unstable nadic end-caps with the phenylethynyl-terminated end-caps, a new material was designated AFR700C or AFR-PEPA-N [2, 3].

### 2.6.3 AFR700C

AFR700C was synthesized in hopes of combining the thermooxidative abilities of AFR700B with the hydrolytic stability of PETI-5 and be able to withstand prolonged temperatures equivalent to AFR700B. This combination is hoped to have the strengths of both materials and yet have no weakness in an hygrothermal environment. Later on the imide oligomer, AFR700C, was termed AFR-PEPA-N due to that it is terminated on

both chain ends with 4-(phenylethynyl) phthalic anhydride, PEPA. The nadic end-cap was removed and no amine groups were left unterminated. The flourinated backbone was kept because of its high thermal properties and hydrolytic stability as seen here in Figure 8[3].

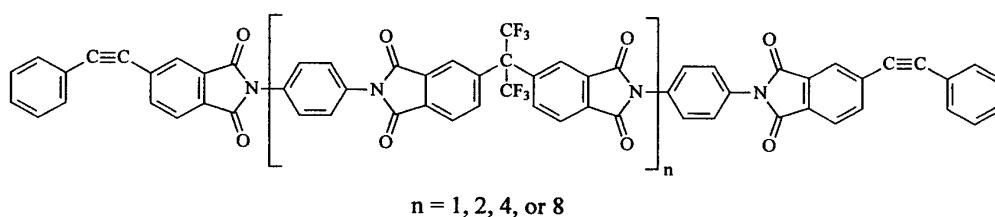


**Figure 8.** AFR-PEPA-N imide oligomer chemical structure, [3].

In the synthesis of AFR-PEPA-N imide oligomer, 4-(phenylethynyl) phthalic anhydride (PEPA), 2,2'-bis(3,4-dicarboxyphenyl) hexafluoropropane dianhydride (6FDA) and para-phenylenediamine (*p*-PDA) were reacted together in N-1Methyl 2 Pyrollidone (NMP). Four imide oligomers were created from this reaction ( $n=1,2,4,8$ ) as seen here in Figure 9[3].

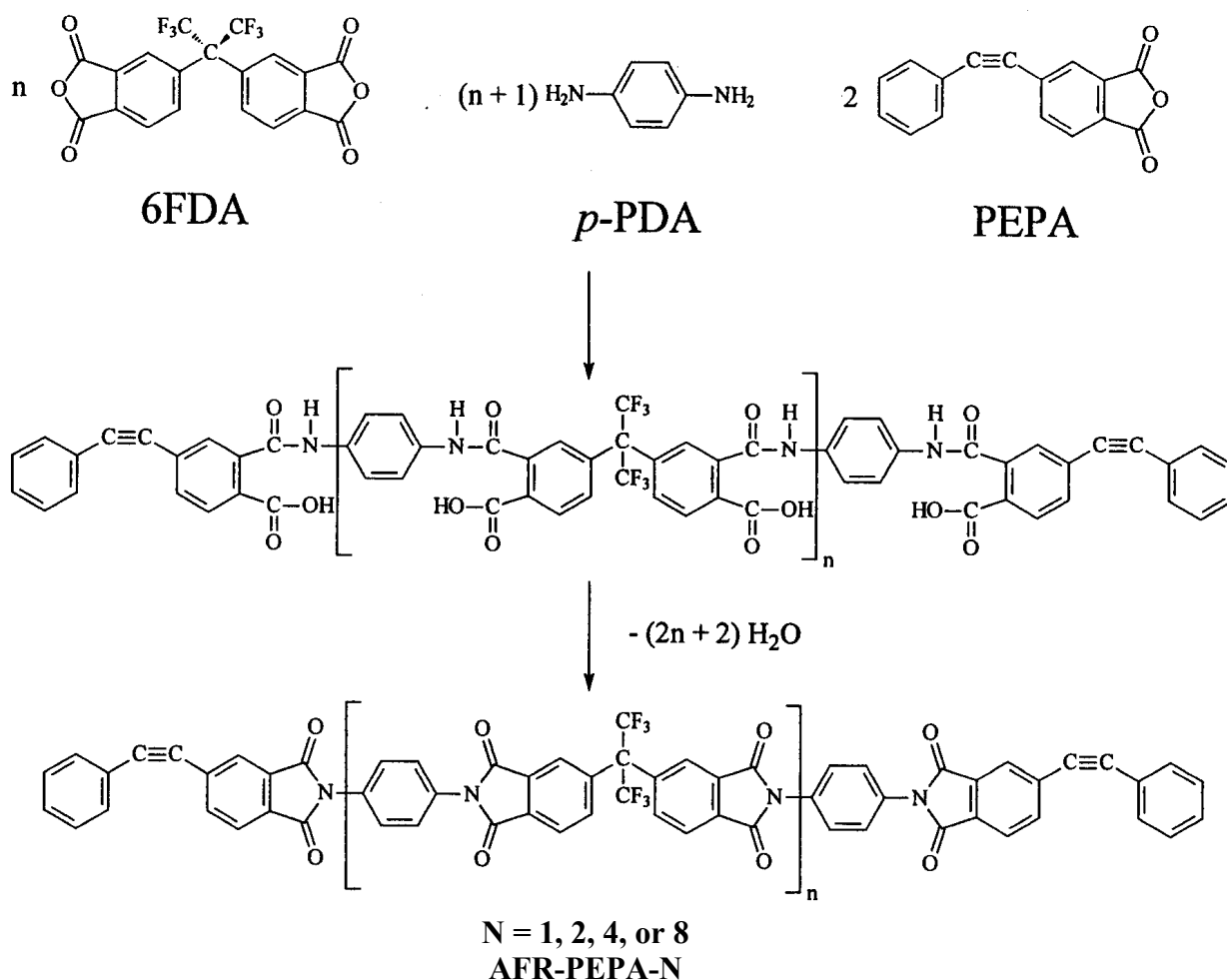


**Figure 9.** Synthesis of AFR-PEPA-N imide oligomers [3].

It was assessed that phenylethynyl terminated AFR700B had  $T_g$ s up to 435 to 455°C. It was found that this polyimide had improved hydrolytic stability relative to the AFR700B. It experienced only a 3 to 5% drop in  $T_g$  compared to AFR700B's 20%

decrease in  $T_g$ , when subjected to a hygrothermal environment. It also had superior mechanical properties compared to AFR700B in a 300°C environment [3].

Lincoln completed several initial characterization studies of the structure-property-processing relationships of the AFR-PEPA-N polyimide. The purpose of these studies was to confirm that this material meets the specifications set out by the United States Air Force. The ultimate goal was to ascertain a material that could be processed by resin transfer molding, display the necessary mechanical properties under a high temperature of 300°C and be hydrolytically and thermooxidatively stable. In detail Lincoln researched the “(i) rheological properties, (ii) mechanical properties, (iii) glass transition temperature, (iv) cure kinetics, (v) thermal stability, and (vi) possible crystallization (as observed in PETI-5) [3].”

The polyimide was found to have superior hydrolytic stability similar to PETI-5 and has excellent mechanical properties at high temperatures. He found that there was a correlation between the mechanical response and crystallinity, but this relationship was not well understood. The viscosity characteristics were acceptable for processability, in some instances, but it was recommended to put additives in the polymer system to lower the polyimide’s viscosity in order to ease processing [3].

#### 2.6.4 Liquid-Crystalline and Rigid-Rod Polymers

Liquid crystalline behavior is the two-dimensional ordering of molecules. The nature of the ordering lies somewhere between the random behavior of a liquid and the three-dimensional ordered crystals of a solid. As mentioned in Section 2.5, there are three types of packing patterns for liquid crystals, (a) nematic (b) cholesteric and (c) smectic [10]. The compositions are determined by the geometric packing of the rods. The alignment also depends on the attractive and repulsive forces from the molecular structure [12].

Liquid crystallinity is due to the behavior of rigid-rod type molecules. The molecular structure is what gives it its rigidity. Dowell predicts that rigidity is based on the “sequence of conjugated aromatic, double and triple bonds in a molecule [12]”. It also can be distinguished by how much the pi-orbitals overlap and the large amount of carbon-carbon bonds.

The liquid-crystalline structure may lead to a more uniformly crosslinked network structure due to the alignment of the oligomer end groups. The liquid crystals could be oriented and when the polymer is cured, the crosslinks will be created along the orientation axis of the crystals. This allows for anisotropic liquid crystalline structure that is a self-assembled structure [7].

For a nematic solution to create a material with a very high, nearly theoretical modulus, the solution must satisfy three requirements: (a) good lateral packing, (b) the rods are nearly flawlessly oriented, and (c) the defects are held at a minimum [13]. For liquid crystalline material to form, the mesogens must orient [14].

Odell et. Al studied the orientability of rigid-rod molecules in solutions using computer modeling programs and experimentally. They found that “the rods are much less hindered in their rotations” than previously thought [15]. Liquid-crystalline thermosets were aligned in a magnetic field by Rozenberg et al. They observed that as the thermoset cured, the polymer decreases in order [16].

The Air Force has put a considerable amount of effort and research into ordered polymer technology. Arnold “uncovered a unique film forming precipitate in the form of a two-dimensional sheet from nematic solutions of PBO and PBT [17]. These were synthesized from a “highly fused aromatic heterocyclic polymer system” for high temperature applications [17].

Lusignea realized the possibilities of applying these unique rigid-rod-like polymer systems. These could be used for “structural, electronic, thermal, and optical” applications [18]. The films could be applied to multi-ply laminates for aerospace applications. PBO and PBZT were found to have excellent capabilities such as a high

tensile strength and modulus, high thermooxidative resistance, self-reinforcing, and were very lightweight relative to other composites. The materials do have a very low compressive strength [18]. It was also found that PBT and PBO have excellent thermal stability and their onset of degradation was at 620°C [19].

Most of the research relies heavily on wide-angle x-ray scattering (WAXS), transmission electron microscopy (TEM), small-angle x-ray scattering (SAXS), and the optical microscope when characterizing liquid crystalline material. WAXS can be used to observe three-dimensional texturing by localized Bragg scattering. SAXS can be used to observe the materials voids. DF imaging is used to find the size and shape of the crystallite [20]. Crystalline oligomers' unit cell was observed by x-ray diffraction while undergoing solid-state transition. The unit cell exhibited contractions under thermal stressing. The crystalline oligomers also exhibited a high melting temperature but a low solubility [21].

Solubility seems to be a problematic issue for liquid-crystalline material. Martin and Thomas concluded, "the solubility of the polymer depends upon the complexity of the backbone [20]." Cheng and Lee observed phase separation when using rigid-rod polymers. To guard against separation, they blended a rigid-rod polymer with a coil-like polymer [22]. Rigid-rod polyimides and PEI were found to be completely miscible due to their similar backbone structure. It was also found that a small amount of rigid-rod

like polymer could be added to increase the tensile modulus of a material by a significant amount [23].

Understanding the possibilities and limitations in manipulating a polymer's chemical structures, to ensure the possibility of liquid-crystallinity, is important in the next steps of developing the high-temperature polyimide. These requirements and procedures could be implemented to modify AFR-PEPA-N so that producing a liquid-crystalline; rigid-rod polymer would be a possibility.



## CHAPTER III

### MORPHOLOGICAL INVESTIGATION OF AFR-PEPA-N IMIDE OLIGOMERS AND THEIR CURED POLYIMIDES

#### 3.1 Introduction

As mentioned in the previous chapter, AFR700B had excellent thermooxidative and toughness properties, however it failed to be a hydrolytically stable material in combine high temperature, pressure, and moisture environments. The AFR700B composite suffered from severe blistering. It was found that only a small amount of moisture, in the AFR700B specimens, was needed to begin the blistering process. Only 0.4-wt.% moisture content was required to initiate blister formation [3].

However, the research did not end there. AFR700B was improved upon, by altering the chemical structure of the polyimide. The nadic end-cap were removed and replaced by, a more hydrolytically stable end-cap. 4-(phenylethynyl) phthalic anhydride, PEPA, was placed at both ends of the backbone, instead of just one end. In the previous design, one nadic end-cap was place on one end of the chain, and an amine was placed at the other end of the chain.

Previous research has found that amines at the ends of polyimide chains can be extremely detrimental to the stability of the polymer. This new end-cap promises a more hydrolytically stable polyimide, while keeping the excellent properties of AFR700B. AFR700C was very successful in the preliminary characterization studies.

From the previous research it has been suggested to further study the relationships between oligomer crystallinity and the properties of phenylethynyl terminated polyimides. This understanding is valuable in processing a polyimide to obtain its optimum properties. The figure below shows the differential scanning calorimetry study that Jason Lincoln performed on AFR-PEPA-2.

In Figure 10, this DSC trace shows the thermal transitions that this imide oligomer experiences when heated from 100°C to 450°C at a rate of 20°C per minute. DSC is a thermal analysis tool used to analyze the characteristics and behavior of most materials. The DSC measures the change in latent heat and heat capacity, over a temperature range. From the change in latent heat, crystallinity, crosslinking temperatures, and melting temperatures can be determined. The glass transition can be found from the change in slope. DSC is not the best tool for determining the glass transition temperature.

The glass transition temperature is shown here before the oligomer is cured. This plot shows the endothermic crystal melting and crosslinking taking place in a small temperature window [3]. During the melting and curing processes the oligomers become less aligned, releasing different amount of energy depending upon the movement when being heated. This figure will aid in understanding how to further study the processing window of the polyimide.

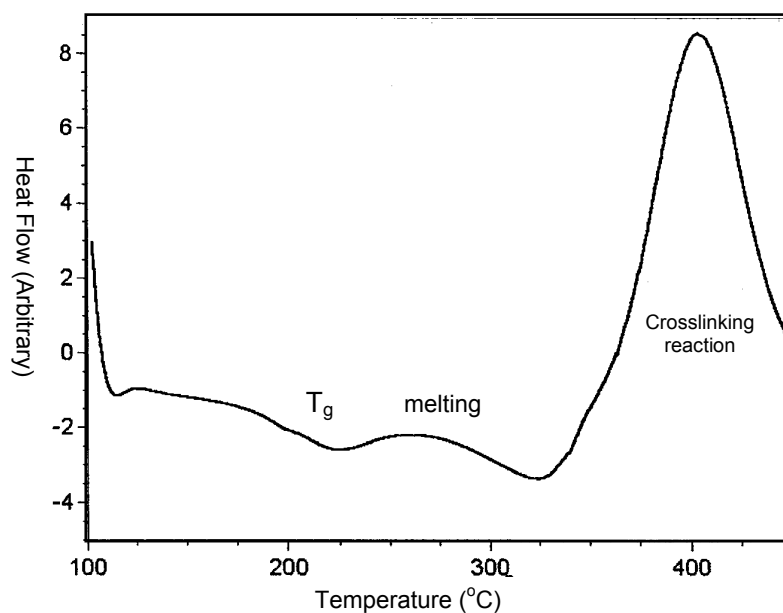


**Figure 10.** Typical DSC trace of imide oligomer at heating rates of  $20^{\circ}\text{C}/\text{min}$  (AFR-PEPA-2) [3].

The objective of this study is to investigate any possible liquid crystalline nature of the precured and cured polyimide oligomer as a function of chemical composition, temperature, molecular weight, and oligomer synthesis conditions, by birefringence. The results from this research will aid in the “optimization of structure-property-processing relationships” of the polyimide for use in resin transfer molding (RTM) of complex shaped composites [6].

This research described in this chapter will focus upon:

- ◆ identification of a reasonable processing window,
- ◆ residual oligomer crystals acting as stress concentrators and initiators of microcracking,
- ◆ a potential temperature overlap between the melting of crystals and the curing of the polyimide,
- ◆ and possible crystalline and/or liquid crystalline characteristics.

## 3.2 Experimental Techniques

The experimental techniques are based upon the layout discussed in Chapter I, Figure 4. These tests are to access the crystal morphology, melting crystal and curing kinetics, and liquid-crystalline behavior.

### 3.2.1 AFR-PEPA-N Imide Oligomer Film

AFR-Pepa-N (-2, -4, -8) were cast into ~0.2 mm thick films onto glass cover slides. In a small glass beaker, the powder was dissolved using N-1Methyl 2 Pyrollidone (NMP). The solution was stirred vigorously for approximately five minutes. A pipet was used to place several drops of the solution on a glass cover slide.

These substrates were heated at 150°C, 200°C, and 250°C, on a Corning Hot Plate – Stirrer, until all of the NMP had evaporated. Using digital temperature readout from carefully placed thermocouple monitored the temperatures. The films were cooled slowly, so that no additional cracking would form from a high thermal gradient. The films were then analyzed under cross-polarized light using the Olympus BX60 optical microscope. Micrographs were taken of the film morphology using FlashPoint FPG, a software package.

### 3.2.2 AFR-PEPA-N Melting and Curing Characterization

The films were then heated over a range of temperatures. The purpose of this test was to understand the melting and curing kinetics of the AFR-Pepa-N system. There is a need to find a large processing window, between oligomer crystal melting and the onset of cure and associated crosslinking, where the best possible chance to implement the resin transfer molding (RTM) process.

The groups of film were annealed in a Lindberg/Blue Oven (courtesy of Dr. Karaman and his research group) at an isotherm of 325°C, 350°C, 355°C, 360°C, or 375°C for fifteen minutes. The films were taken out of the oven immediately, and the crystal structure was characterized under polarized light using the Olympus BX60 optical microscope. As before, micrographs were taken of the new film morphology using FlashPoint FPG.

Also other film was heated with respect to temperature and time and the morphology was analyzed in real time. The film substrate is placed onto a heating element within the Mettler FP84 Thermal Analysis Microscopy Cell. This equipment allows light to pass through the element so that the heated substrate could be monitored by optical microscopy. The Mettler FP80 Central Processor is programmed to start at

150°C and increase up to 10°C per minute. It will shut off at 375°C. Over this time, the morphology of the film will be observed using the Olympus BX60 optical microscope.

### 3.2.3 AFR-PEPA-N Ratio Film

A molar mass-based ratio of Pepa-4 and Pepa-8 was prepared. It was observed that Pepa-8 does not contain any crystals unlike Pepa-2 and Pepa-4 under the polarizing microscope. Unfortunately AFR-PEPA-8 cannot be processed because its viscosity is extremely high. It was decided to create a blend of PEPA-8 and PEPA-4 in hopes that the PEPA-8 would terminate the nucleation of crystals, yet the presence of PEPA-4 would decrease the viscosity.

A 50:50 and a 25:75 ratio of Pepa-4 and Pepa-8 were blended together, and the films were cast from the mixtures using the same methods as previously described in Section 3.2.1. The crystalline morphology of the films was studied at under cross-polarized light using the Olympus BX60 optical microscope.

### 3.2.4 Crystal Dissolution Characterization

The Pepa-2 oligomer powder was vigorously stirred in N-Methyl 2-pyrrolidone for approximately five minutes at room temperature. The solution was observed under

cross-polarized light using the Olympus BX60 optical microscope. Undissolved powder crystals were found from these observations shown in Figure 11.

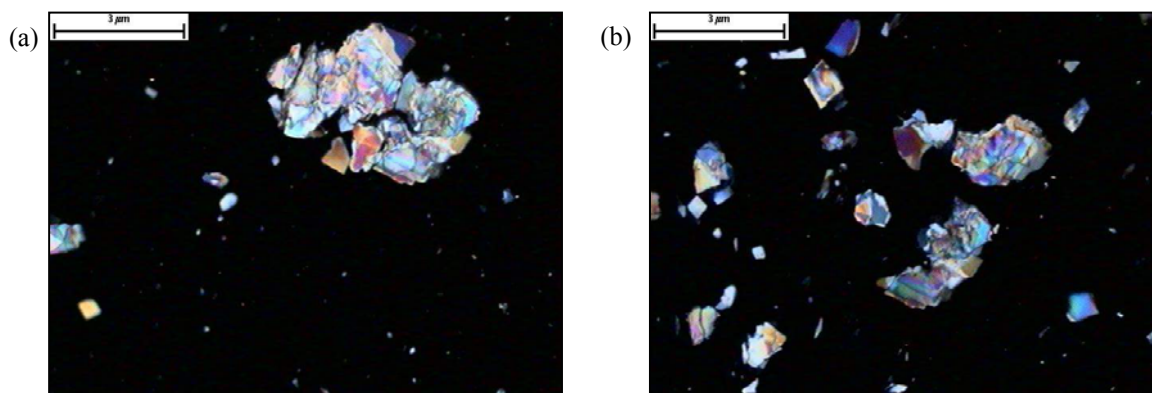


**Figure 11.** (a) Micrograph of AFR-PEPA-2 imide oligomer powder in NMP at room temperature, undissolved oligomer crystals. (b) Micrograph of AFR-PEPA-2 imide oligomer powder in NMP at room temperature: same crystals that are stressed and broken up.

Several tests were run to see if the oligomer would dissolve under a certain circumstances and constraints. A low concentrated solution (1 gram to 1 L) was blended for 24 hours at room temperature in a round bottom flask with a Teflon® coated stir bar. Several other solutions were run for different times and temperatures using a Glas-Col Series O Heating Mantle and a round bottom flask with a Teflon® coated stir bar. The systematic tests are shown below in Table 2.

Samples were taken from the solution and monitored under cross-polarized light by the Olympus BX60 optical microscope. Micrographs that describe the general makeup of the crystals within the solution were taken using FlashPoint FPG. Crystal



sizes were measured from each solution using these micrographs. The measurements were used to compare how well the crystals dissolved into the N-Methyl 2-pyrrolidone.

*Table 2. Dissolution tests as a function of time and temperature.*

<b>Dissolution Tests</b>	
<i>1</i>	5 minutes at 23°C
<i>2</i>	24 hrs. at 23°C
<i>3</i>	24 hrs. at 60°C
<i>4</i>	72 hrs. at 50°C
<i>5</i>	72 hrs. at 50°C; Ground
<i>6</i>	24 hrs. at 100°C

### 3.2.5 Liquid Crystal Characterization

The films are stressed under the optical microscope, with cross-polarized light, in order to identify any of these unique liquid-crystalline patterns that were shown previously in Chapter II, Section 5. A ‘shear’ test was conducted to ascertain for any liquid crystalline nature in the Pepa-2 film specimens. The films are cast using the same method for the previous tests in Section 3.2.1. We investigated for any shear banding that appeared under cross-polarized light. Figure 12 shows the manner in which the characterization procedure was set up. Two Pepa-2 film specimens were used for the shear test. Specimens were sheared at 360°C, above the oligomer crystal melting point, after being exposed to this temperature for (i) five minutes and (ii) fifteen minutes. A 0.025-in thick aluminum sheet substrate was used because of its high thermal conductivity. As seen in Figure 12, a groove was cut out of the aluminum sheet.

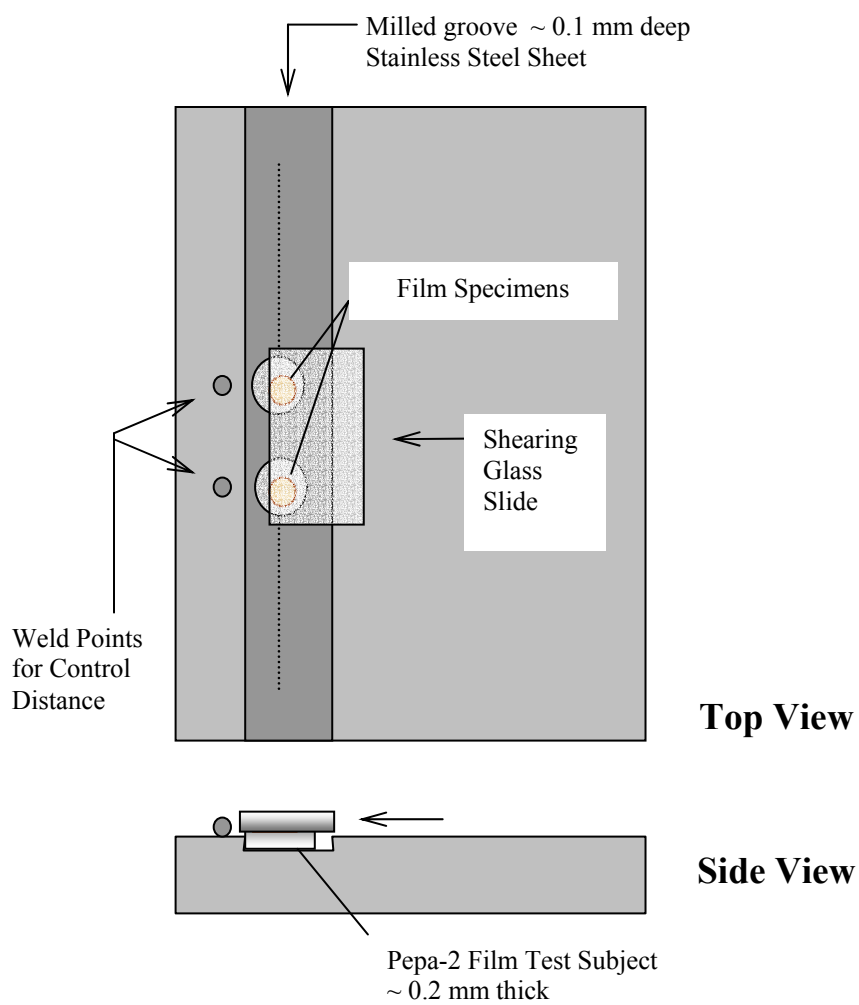


**Figure 12.** *Shear experimental apparatus setup.*

This groove held the film firmly enough so that the slide, when moved across the film, did not drag the specimen along with it. The groove was 0.007-in which was slightly shallower than the 0.010-mm glass cover the film was on. The furnace temperature was set at 360°C. The film has a low viscosity at the isotherm. The low viscosity allows the glass slide to shear the film with as little adhesion as possible.

After the film was exposed to the temperature, for a specific amount of time, the slide was forced over the film substrate. This applied stress may cause alignment of the molecular rods, if the polyimide is in liquid-crystalline phase. The alignment may be observed using the cross-polarized light from the optical microscope.

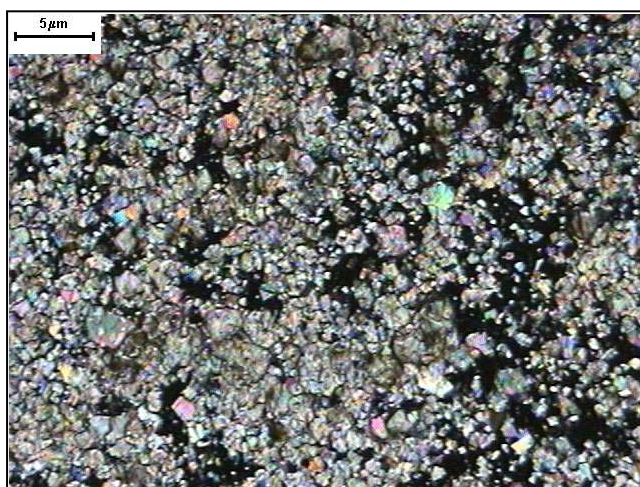
### 3.3 Results and Discussion

#### 3.3.1 Crystal Structure and Morphology Results

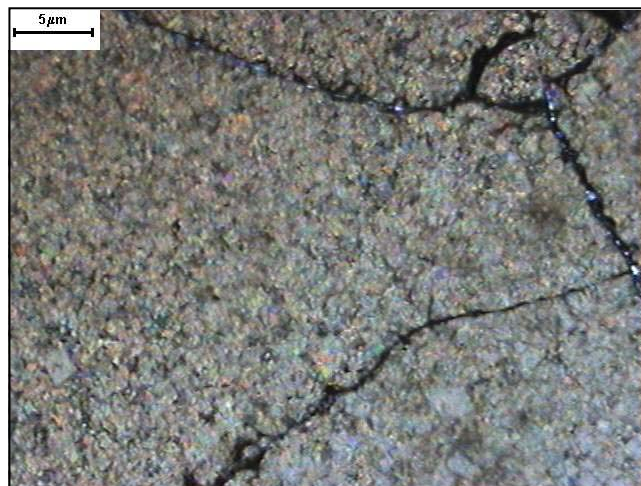
Films were cast prior to the knowledge of the solubility problem associated with the AFR-PEPA-N imide dissolving into NMP. Crystals were found in the Pepa-2 and Pepa-4 films at all of the processing temperatures. There were no crystals present in all of the Pepa-8 film. Microcracking was observed in all of the films. The cracking is due to the thermal stresses experienced during the processing of the films.

##### 3.3.1.1 *Crystal Size as a Function of Imide and Temperature*

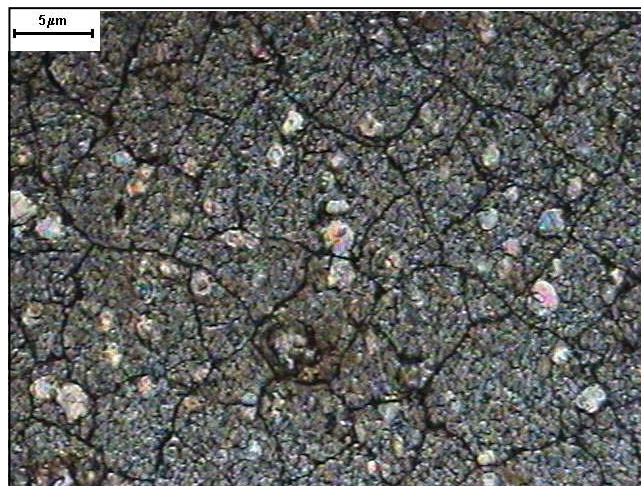
Optical micrographs were taken of the films at each annealing-processing temperature. Figures 13 and Figure 14 show AFR-PEPA-2 and AFR-PEPA-4 imide oligomer film morphology that were cast at each different temperature and then viewed at room temperature. The pictures do vary from each other due to variations in concentration, however the crystals seemed to have similar shapes for each temperature exposure and imide oligomer. One interesting observation is that in most of the pictographs of the film, there are several large crystals surrounded by a large crowd of small crystals.



Cast at  $T = 150^{\circ}\text{C}$   
Average Crystal  
Length =  $0.825\ \mu\text{m}$

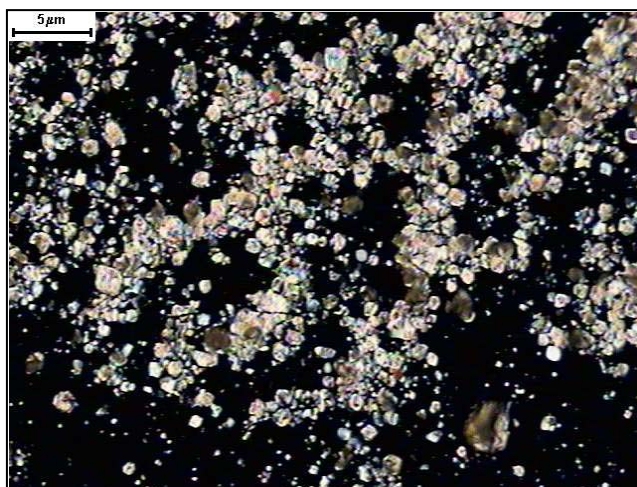


Cast at  $T = 200^{\circ}\text{C}$   
Average Crystal  
Length =  $0.907\ \mu\text{m}$

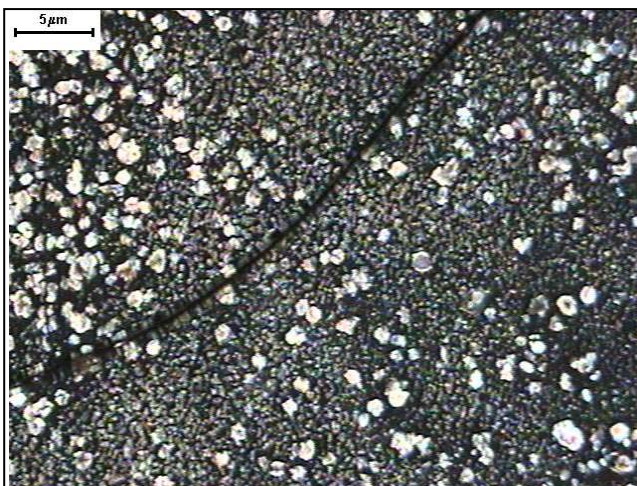


Cast at  $T = 250^{\circ}\text{C}$   
Average Crystal  
Length =  $0.645\ \mu\text{m}$

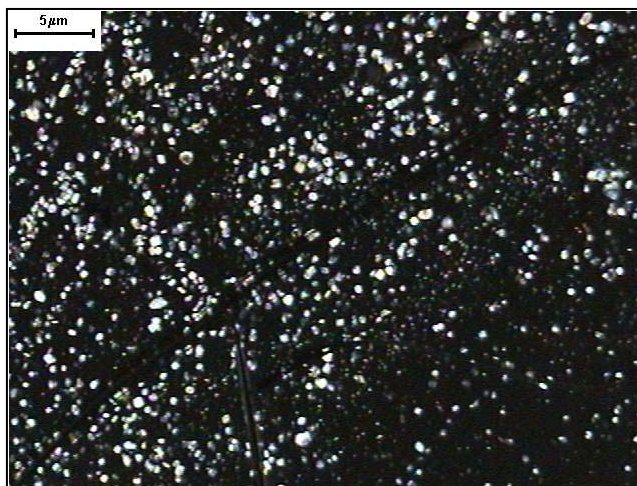
**Figure 13.** AFR-PEPA-2 imide oligomer film morphology with average crystal length as function of temperature, viewed at room temperature.



Cast at  $T = 150^{\circ}\text{C}$   
Average Crystal  
Length =  $1.134\ \mu\text{m}$



Cast at  $T = 200^{\circ}\text{C}$   
Average Crystal  
Length =  $0.696\ \mu\text{m}$



Cast at  $T = 250^{\circ}\text{C}$   
Average Crystal  
Length =  $1.459\ \mu\text{m}$

**Figure 14.** AFR-PEPA-4 imide oligomer film morphology with average crystal size as function of temperature, viewed at room temperature.

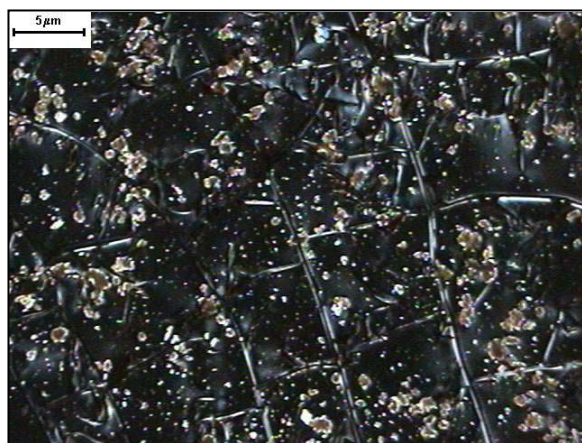
Approximately a sample size of twenty crystals was randomly selected from a representative picture from the films. A single crystal's largest dimension and shortest dimension were measured and averaged. The measurements were then averaged. Table 3 for Pepa-2 and Pepa-4 shows the crystals sizes of the film at the different processing temperatures. There appears to be no consistent dimensional change with annealing temperature.

**Table 3. Crystal dimensions as a function of oligomer and processing temperature.**

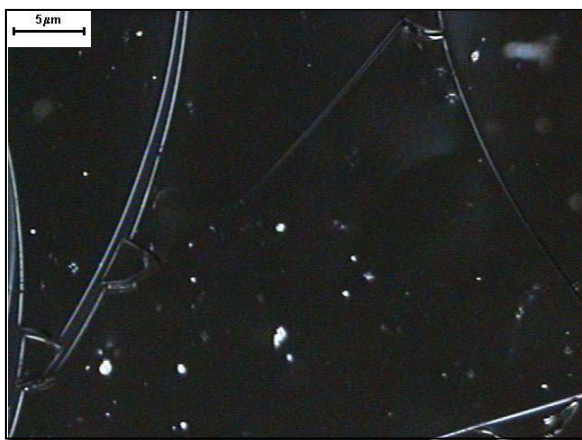
<b>Pepa-2</b>		
Temperature	Averaged Length ( $\mu\text{m}$ )	Area ( $\mu\text{m}^2$ )
150°C	0.825	0.535
200°C	0.907	0.646
250°C	0.645	0.328
<b>Pepa-4</b>		
Temperature	Length ( $\mu\text{m}$ )	Area ( $\mu\text{m}^2$ )
150°C	1.134	1.010
200°C	0.696	0.380
250°C	1.459	1.671

In Figure 15, AFR-PEPA-8 showed an interesting morphology at each temperature. At 150°C, there were small brown clumps scattered throughout the film. These seem to have been undissolved oligomer powder that were 'frozen' into the film. At 200°C and 250°C, there are no brown clumps noticed, however there are several

'crystal-like' forms. This could be contamination, but overall there were no large amount crystal forms relative to the AFR-PEPA-2 and AFR-PEPA-4 films.



Cast at T = 150°C



Cast at T = 200°C

**Figure 15.** AFR-PEPA-8 imide oligomer film morphology cast at different isotherms and viewed at room temperature.



### 3.3.1.2 *Ratio-Morphology*

Pepa-4 and Pepa-8 were blended at different ratios of 50-50 and 25-75 to achieve a low viscosity polyimide with no crystals present. This could potentially achieve a large enough processing window where there would be ample time to make a quality product via RTM. These films were also viewed in the polarizing optical microscope at room temperature. The micrograph of each ratio is shown in Figure 16 and Figure 17.

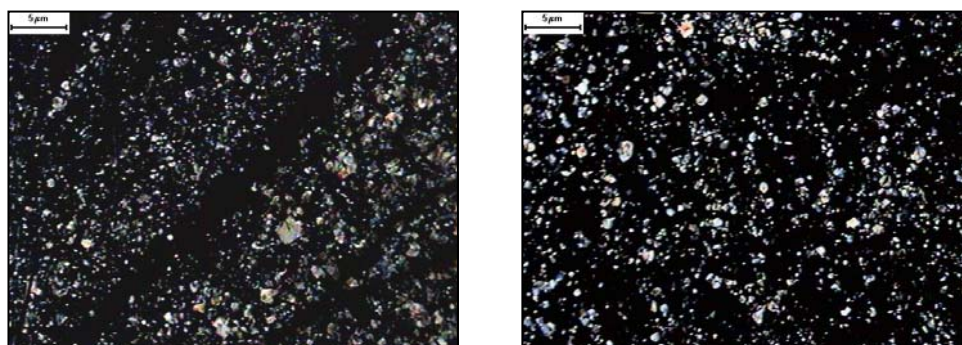


**Figure 16.** 50-50 Ratio of AFR-PEPA-4 and AFR-PEPA-8.

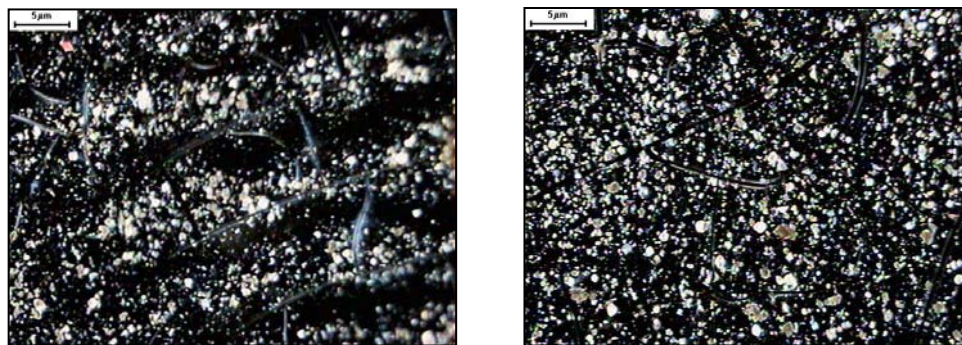


**Figure 17.** 75% AFR-PEPA-8 combined with 25% AFR-PEPA-4.

Unfortunately, the film did not show any significant changes relative to the Pepa-4 film. It still contained a large amount of crystals and had a similar appearance to Pepa-4 and Pepa-2. From these results we can infer that Pepa-8 and Pepa-4 are becoming mutually immiscible. As can be seen in Figure 16 and Figure 17, both ratio blends contain a high concentration of crystals.

The left micrograph, of both Figure 16 and Figure 17, shows a separation between bands of crystals. This separation may be due to the presence of AFR-PEPA-8 imide oligomer in the blend. Results from the rheological tests completed by Lincoln et. al. [3] conclude that the mixing of the ratios do not give the desired processing viscosity appropriate for RTM.

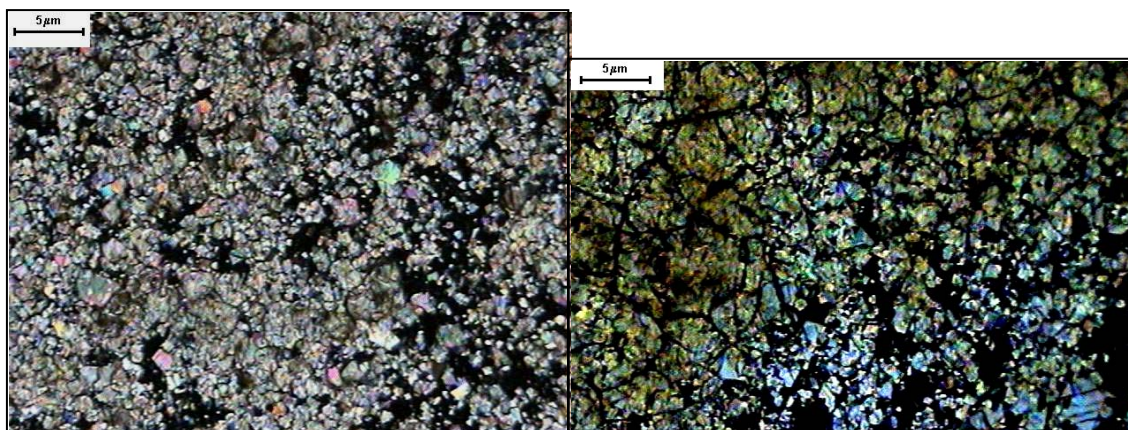
### 3.3.2 Furnace Curing Results

***Table 4. Observed oligomer film morphology at different annealing temperatures.***

<b>Curing Isotherm at 15 minutes (°C)</b>	<b>Film Morphology under Cross-Polarized Light Optical Microscope</b>
325	No discernable melting, microcracks widen.
350	Crystal Melting observed
355	Still are a large amount of crystals present; most of the smaller crystals have melted.
360	Most crystals melted.
375	Few crystals observed.

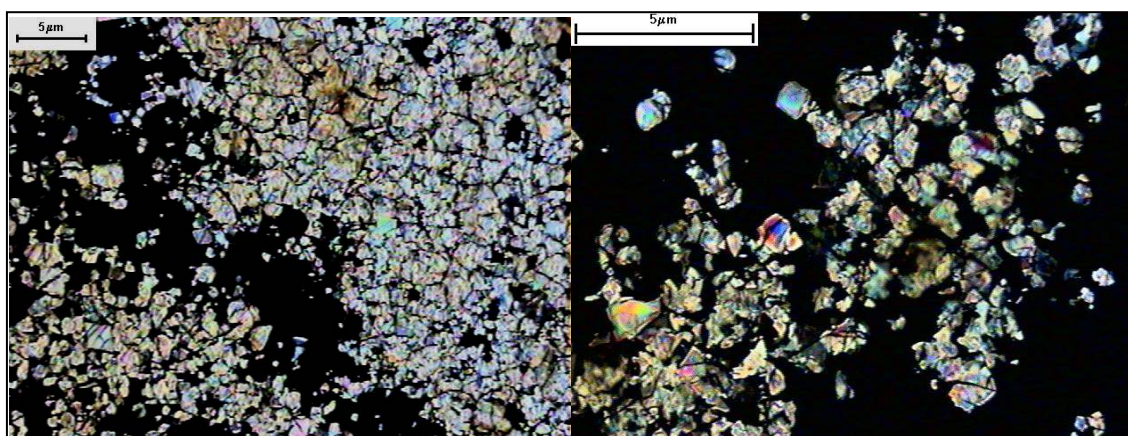
Table 4 gives a brief synopsis of the crystal behavior at each isotherm. We observed that the larger crystals took a higher annealing temperature to melt, which will decrease the processing window. If the crystals do not completely melt fast enough, the material will crosslink with several crystal defects in the matrix. If the crystal size can be reduced, the processing window to melt the crystals could significantly widen.

In Figure 18, these pictographs show the film morphology change at each different isotherm. These processed films were viewed via polarizing optical microscope at room temperature. From Figure 18(a) to Figure 18(b) there seems to be no development of amorphous regions nor any signs of crystal melting. A dramatic change is noticed between Figure 18(c) and Figure 18(e). The film that was cured at 355°C was to establish a gradual change between these two isotherms. From Figure 18(d), the smaller crystals begin to melt between 350 and 355°C. The melting occurs at the edges of the crystal groupings and slowly works its way to the center of the crystal clusters. The clusters ‘break up’ and the melting occurs at a faster rate. This rate is noticed by the dramatic difference between Figure 18(d) and Figure 18(e). In Figure 18(f), there is only one or two crystals remaining within the completely crosslinked material. Another interesting artifact to note is the wisp-like characteristics in Figure 18(e). These wisps were found in most of the film at this specific temperature. This could be evidence of liquid-crystalline behavior. This specific type is similar to Figure 5(a) in Chapter II, which shows that there would nematic behavior in this material.



(a) No Anneal / Cure: Film cast at 150°C.

(b) Cure at 325°C, 15 minutes.



(c) Cure at 350°C, 15 minutes.

(d) Cure at 355°C, 15 minutes.

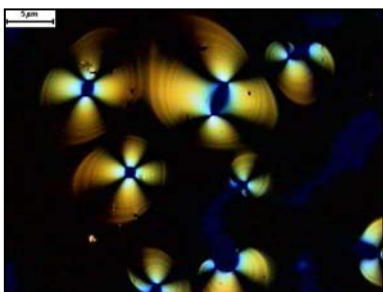


(e) Cure at 360°C, 15 minutes.

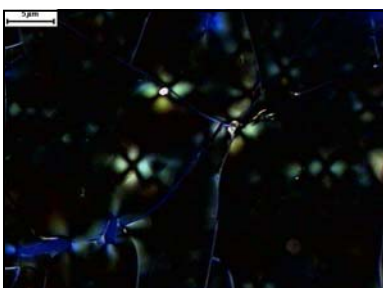
(f) Cure at 375°C, 15 minutes.

**Figure 18.** AFR-PEPA-2 film morphology at varying isotherms held at fifteen minutes each, viewed at room temperature (a-f).

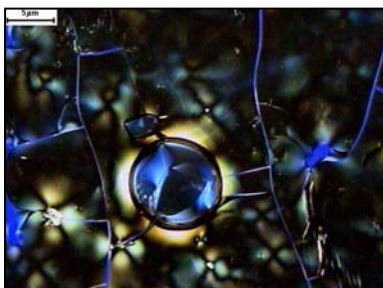
The cure at 360°C produced interesting artifacts in the film shown in Figure 19. Some of these could be evidence of nematic liquid-crystalline behavior.



PEPA-2, 200°C, cured at 360°C.



PEPA-4, 200°C, cured at 360°C



PEPA-4, 200°C, cured at 360°C.

**Figure 19.** *Liquid-crystalline behavior at 360°C cure for both PEPA-2 and PEPA-4, viewed at room temperature.*

### 3.3.3 Shear Test Results

After being heated in the Lindberg/Blue oven at 360°C, for five minutes, the film substrates were manually sheared in the oven, as shown in Section 3.2. The films were viewed at room temperature via the polarizing optical microscope. In Figure 20, AFR-PEPA-2 is shown to have one or two places where shear banding occurred.

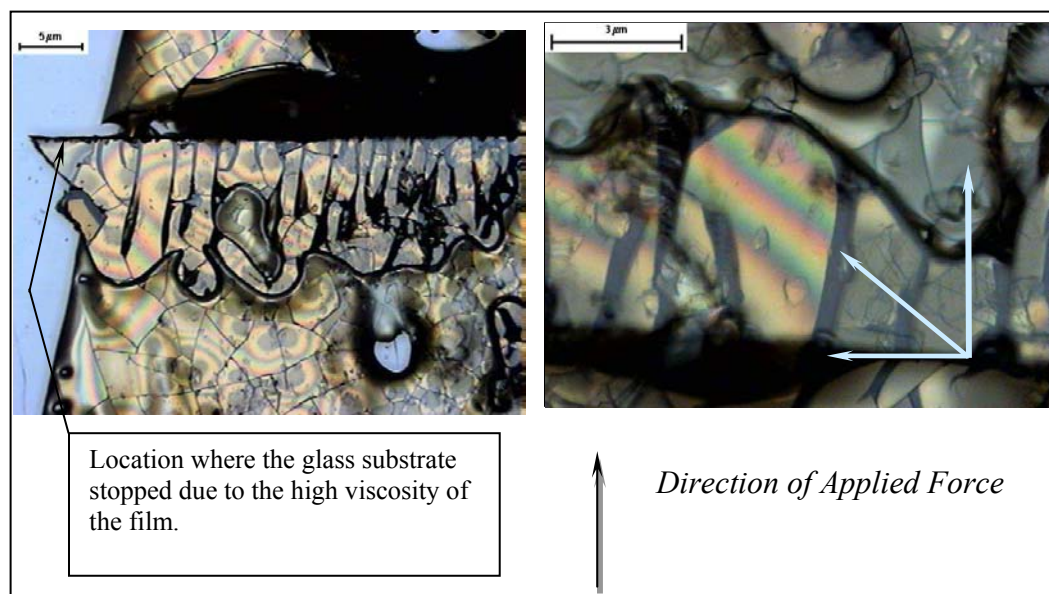


**Figure 20.** AFR-PEPA-2 film morphology result of manually applied shear, viewed at room temperature.

This is where bands occur that is approximately 45° from the direction of the applied force. However, looking at the overall picture (on the left), the bands do not follow this direction, but change direction in every piece of the film. There are significant signs of liquid-crystalline behavior from previous crystal morphology studies in Section 3.3.2. The figure showed no consistency in the banding. This would lead us

to the conclusion that the liquid-crystalline behavior is not as ordered as it could be. It may contain nematic liquid crystals.

### 3.3.4 X-Ray Results

The purpose of the x-ray diffraction test was to assure what was being observed visually in the optical microscope was, in fact a crystalline structure. The oligomer unit cell is observed using a wide-angle x-ray diffraction technique.

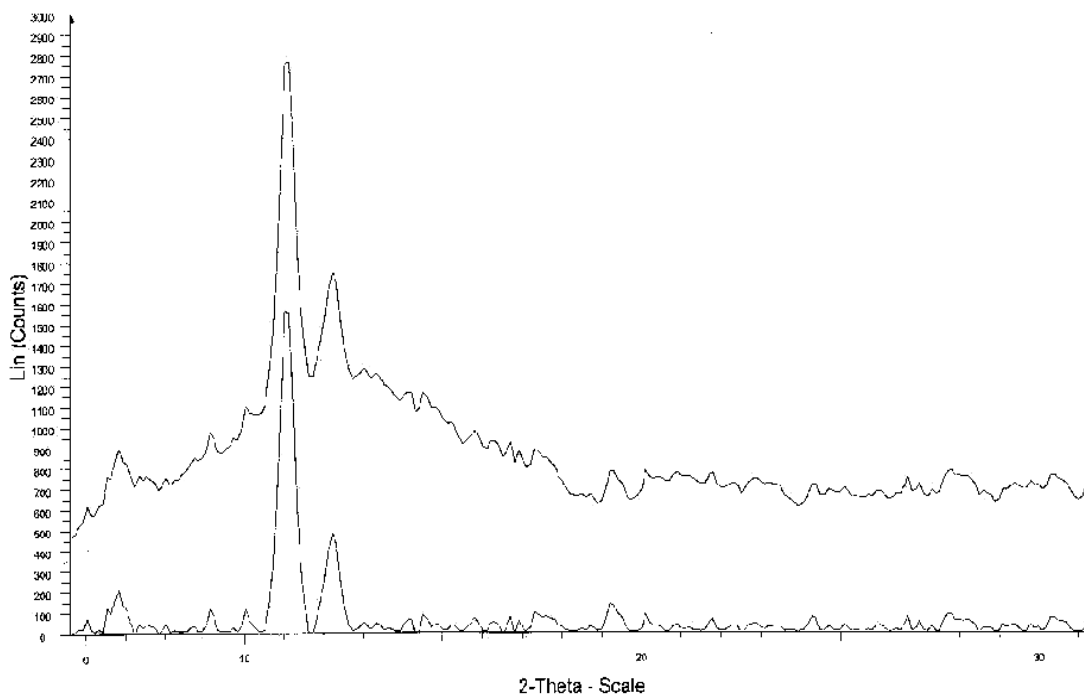


**Figure 21.** Wide-angle x-ray diffraction plot of AFR-PEPA-2 film.

The wide-angle x-ray diffraction test shows, in Figure 21, that there was evidence of crystallinity in the AFR-PEPA-2 film. The d-spacing ranged between seven

and eight Angstroms. The graph shows two predominate peaks, which indicate the crystallinity in the specimen.

### 3.3.5 Solubility Results

After it was discovered that the crystals were innate in the powder form of the AFR-PEPA-N, dissolution tests were conducted to find at what circumstances the powder dissolved completely.



**Figure 22.** *AFR-PEPA-2 imide oligomer: 0.01 g / 10mL NMP blended for 24 hr. at 23°C.*

At 24 hours at room temperature, a concentration of 0.01 gram of AFR-PEPA-2 was blended with 10 ml of NMP. Figure 22 shows that there is still a small quantity of crystals remaining in the low concentrated solution. However, this is a significant reduction in the amount of crystals relative to a solution blended for several minutes.



At 24 hours at 100°C for a concentration of 0.01 gram into 10 ml, it was found that the Pepa-2 powder completely dissolved. From here film was cast at 200°C and 250°C. There were no crystals found in either film. From this observation, it was realized that the crystals from the prior films were produced not by the heating of the solutions, but were inherent from the formation of the oligomers.

This discovery potentially opens the processing window widely, without concern of crystals creating defects in the crosslinked structure. If the crystals cannot be completely dissolved at higher concentrations, the crystal size can be reduced to a certain degree. There could be a link between smaller crystal size and a widened processing window.

### 3.4 Conclusions

- ◆ The initial results show that the crystal melting occurs between a small processing window of 350°C and 360°C. There is approximately 50% cure at 355°C for fifteen minutes. The material cures completely by 371°C. From these initial results, the processing window is very small and cannot produce a fully cross-linked material free of crystal defects. It is also concluded that larger crystals take more time to melt, than the smaller surrounding crystals. If the overall crystal size can be reduced the melting can be effectively complete before the material crosslinks.
- ◆ If not properly dissolved, Pepa-2 and Pepa-4 oligomer's inherent crystals do not melt quickly enough, giving undesirable defects in the final crosslinked product. However, if the oligomer is completely dissolved, the processing window is greatly widened, allowing a more complete crosslinked matrix with no defects. A solution of 1 gm with 10 ml of NMP, blended at 100°C for 24 hours, is completely dissolved. If a higher concentrated solution is desired, the solution will have to be blended for a longer period of time. However, not all of the crystals need to be dissolved to create a defect-free material. If the crystal size is reduced initially in the dissolving stage, the film's small crystals will melt before the material becomes fully crosslinked.

- ◆ There is optical microscope evidence to conclude that AFR-PEPA-N oligomers have liquid-crystalline behavior, however the nematic liquid-crystalline behavior is weak. That is there is room for great improvement for the higher, ordering of the oligomer rods. This may be due to its bulky chemical structure. Since AFR-PEPA-N has liquid-crystalline characteristics, the structure will need to be improved upon in order to achieve a higher ordered liquid-crystalline form.

## CHAPTER IV

### REMODIFICATION OF AFR-PEPA-N TO ACHIEVE LIQUID-CRYSTALLINE BEHAVIOR

#### 4.1 Introduction

As mentioned in the previous chapter, AFR-PEPA-N establishes itself as a high temperature polymer that has hydrolytic and thermooxidative stability. It can be processed if the concentrations are made correctly. It acts as a thermotropic, nematic liquid-crystalline polymer (LCP) at 360°C. However it does not display a very highly-ordered liquid-crystalline behavior. It has been suggested to make several modifications to the structure of AFR-PEPA-N to achieve a highly-ordered LCP.

The purpose of creating a highly-ordered LCP structure is to attain equal-length, rigid-rod segments that are nearly flawlessly oriented in a particular direction with little to no defects within the system. This structure is represented in Figure 23. The new structure development is to in effect allow the polyimide to have an equal-length, rigid-rod oligomer.

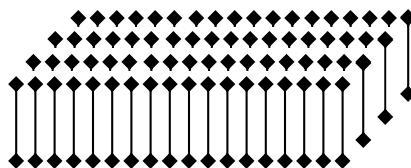


*Figure 23. Morphology of self-assembled rigid-rod oligomers.*

This structure may lead to a more uniformly crosslinked network structure due to the alignment and self-assembly of the oligomer end groups. The rods could be oriented, either by force or by a magnetic or electric field. The rods could also self-align via ionic salts placed in the oligomer end-groups. After self-assembly, the crosslinks would form along the orientation axes of the oligomer end-groups. This anisotropy produces exceptional mechanical, thermal, optical and electrical properties. Each rod would experience an equal load amount, therefore eliminating any stress-raisers. Thus this would create a material with a near theoretical physical properties. These new materials should have superior thermal and mechanical properties relative to the other polymeric materials currently available.

A new ultra-high temperature polyimide needs to be developed from the modifications to AFR-PEPA-N's chemical structure in order to achieve a higher potential for liquid crystallinity. The objective of this research was to first modify the backbone structure of AFR-PEPA-N. Later development will include modifications by introducing an acetylene reactive group and substituting the hydrogen with a magnesium or lithium metal.

The 6FDA fluorine groups give the polyimide a high level of stability; however, these groups are non-linear and exceedingly bulky. It has been suggested that this bulkiness is one particular reason the rods do not align properly. The fluorine groups repel other rods quite possibly due to the fluorine atoms' low polarity. Fluorinated polyimides typically have disadvantages in adhering to different substrates due to this low polarity of the fluorine atom [4].

It has been suggested to replace this bulky monomer, with a more stiff and co-linear monomer. As mentioned briefly in Section 2.5, an aromatic dianhydride, pyromellitic dianhydride (PMDA), is a very stiff and stable monomer. It “is the most reactive” out of all dianhydrides due to its strong electron accepting properties [4]. PMDA might allow for liquid-crystalline attributes, as mentioned in previous research there has been strong evidence that PMDA creates semi-crystalline type polyimides and quite possibly liquid-crystalline polyimides as well.

## 4.2 Experimental Technique

The synthesis involved reacts an aromatic diamine, *para*-phenyldiamine (*p*-PDA), to an aromatic dianhydride, pyromellitic dianhydride (PMDA), and is capped with 4-(phenylethynyl) phthalic anhydride (PEPA), a reactive endgroup in N-methylpyrrolidinone (NMP). PMDA and *p*-PDA both exhibit a co-linear structure that is more suitable for liquid-crystalline characteristics. Their chemical structures are displayed in Figure 24.

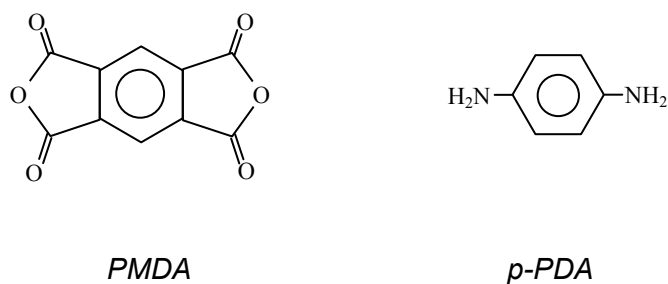


**Figure 24.** Co-linear chemical structure exhibited by PMDA and *p*-PDA.

### 4.2.1 Synthesis Preparation

The 97% pure pyromellitic dianhydride (PMDA), 1,2,4,5-benzenetetracarboxylic dianhydride, from Aldrich, was dried under vacuum at 100°C for 24 hours.

*Para*-phenylenediamine (*p*-PDA) flakes were purchased from Spectrum Quality Products, Inc.; Lot number MJ0071 and is 98% pure. 4-(phenylethynyl) phthalic anhydride, PEPA, was obtained through the Air Force Research Laboratory / Wright-Patterson Air Force Base. Its melting temperature is at 157°C and it becomes volatile around 350°C. It was dried for 24 hours at 60°C in a vacuum oven. N-1 Methyl 2 Pyrollidone (NMP) was the solvent used for the dissolution of the monomers.

#### 4.2.2 Synthesis Procedure

The monomers solutions were measured 10% solids by weight. A molar ratio of 1:1 for PMDA and *p*-PDA was used, and two PEPA was measured. In a three-necked round bottom flask, a solution of *p*-PDA and NMP under a nitrogen atmosphere and stirred at room temperature, using a Teflon® coated stir-bar, until the *p*-PDA is completely dissolved.



Another solution is made combining PMDA with NMP in a nitrogen atmosphere at room temperature. After this powder is completely dissolved, the solution is added to the *p*-PDA at one-third portion each hour. The exothermic reaction is monitored by a thermocouple and is not allowed to exceed 60°C. The solution is continued mixing for twenty more hours at room temperature and in a nitrogen atmosphere. This results in the generation of polyamic acid with NMP.

After the PEPA is removed from the oven, it is added as a solid into the PMDA/*p*-PDA solution still under a nitrogen atmosphere at room temperature. This is blended for four hours. The solution is poured into a beaker and is heated in a vacuum oven at 185°C for twelve hours. This is to remove the water and imidize the polyamic acid. From this the mixture should be in a slurry-type form. The mixture is added to distilled water, filtered and then washed in boiling water. Warm methanol is added and filtered to remove the NMP. The remainder is dried under vacuum for 24 hours at 200°C. This yielded a light-brown powder. The synthesis of TAMU-P3-1 is shown below in Figure 25.

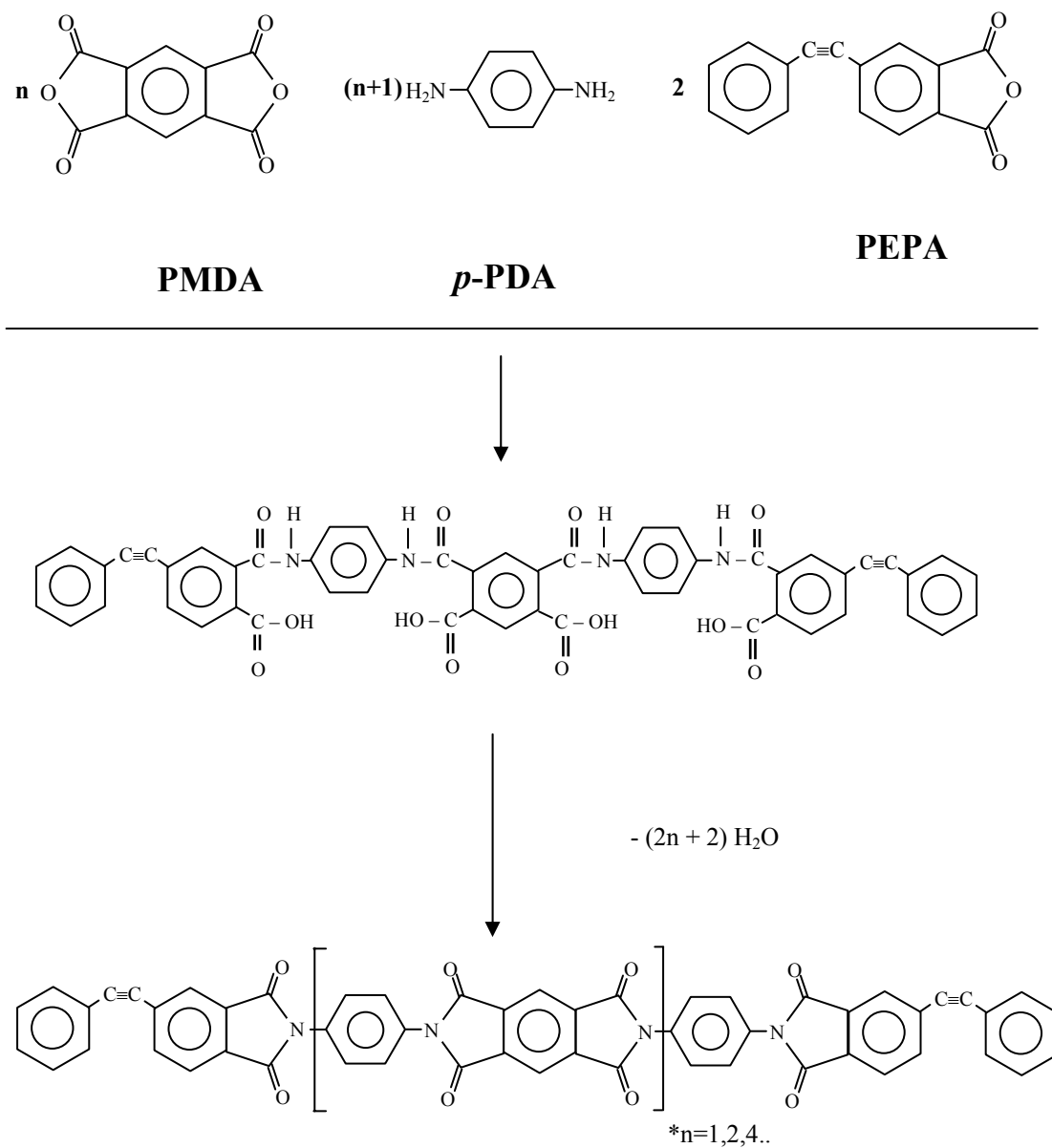


**Figure 25.** Synthesis of TAMU-P3-N.

### 4.2.3 Initial Characterization

Several initial tests were conducted in order to find out if the synthesis was successful and to characterize the new oligomer. A Fourier Transform Infrared test, a Differential Scanning Calorimetry test, and dissolution test were conducted. Below is a description of how each test was conducted and what was desired from each test.

#### *4.2.3.1 Differential Scanning Calorimetry (DSC)*

The Differential Scanning Calorimetry (DSC) technique employs the endothermic or exothermic processes the material experiences as to measure critical points that the specimen may contain. The DSC compares the specimen to an empty reference pan and heats the specimen to a desired temperature over time and the temperature difference is measured through the use of thermocouples.

The TAMU-P3-1 oligomer powder was measured out to be ~5 mg and placed in a tin plate. The test was run using the Perkin Elmer Pyris 1: DSC machine-, from 25°C to 500°C at a rate of 10°C per minute and then at 20°C per minute.

#### 4.2.3.2 *Fourier Transform Infrared (FTIR)*

The Fourier Transform Infrared (FTIR) test essentially emits a beam towards the specimen. The beam interacts with the bonds in the specimen and a resultant beam is collected. The FTIR scan gives a ‘fingerprint’ of the chemical bonding within the test specimen. The resultant peaks are at a particular intensity and wavelength. The type of bonding can be inferred from these intensities and wavelengths. Thus, the polymer synthesis can be found to be a success or not based upon the bonding discovered from the FTIR scans.

Roughly 2 mg of TAMU-P3-1 are finely ground in a mortar and pestle with 100 mg of ground KBr. This is layered into a mini-press and a thin film disk is pressed and placed into the Nicolet Avatar 360 FT-IR E.S.P. machine. A FTIR spectrum was gathered from the original specimen by the EZ Omni E.S.P. data collection computer program. To observe the carbon-triple bond decreasing as the crosslinking increased; FTIR scans were taken of the material to the point of full cure. To accomplish this task, the disks were heated in Lindberg/Blue furnace near the curing temperature. Each film was kept in the furnace at a certain amount of time. A spectrum was produced for each disk exposed to the high temperature over a certain amount of time and compared to its original spectrum obtained prior the curing time.

#### 4.2.3.3 *Dissolution and Liquid-Crystalline Test*

A 1gm-1L ratio of TAMU-P3-1 / NMP was blended in a round bottom flask for approximately one hour at room temperature. The solution was observed under the polarizing Olympus BX60 optical microscope. The solution was cast onto circular cover glasses and heated to 150°C as to evaporate the NMP and leave behind a thin film of TAMU-P3-1. The film was then heated from room temperature to 360°C with a Mettler FP80 heating stage and processor and observed in real time using the polarizing optical microscope.

### **4.3 Results and Discussion**

#### 4.3.1 Differential Scanning Calorimetry (DSC) Results

This section will cover the results from initial tests described in the previous section. Firstly, the results from the DSC test are crucial because that result determines how each other test will be run and what should be looked for. In Figure 26, the DSC test showed an endothermic peak at 351°C. This displays that a certain amount of curing is taking place. At a higher rate of 20°C per minute, the peak becomes more prominent.

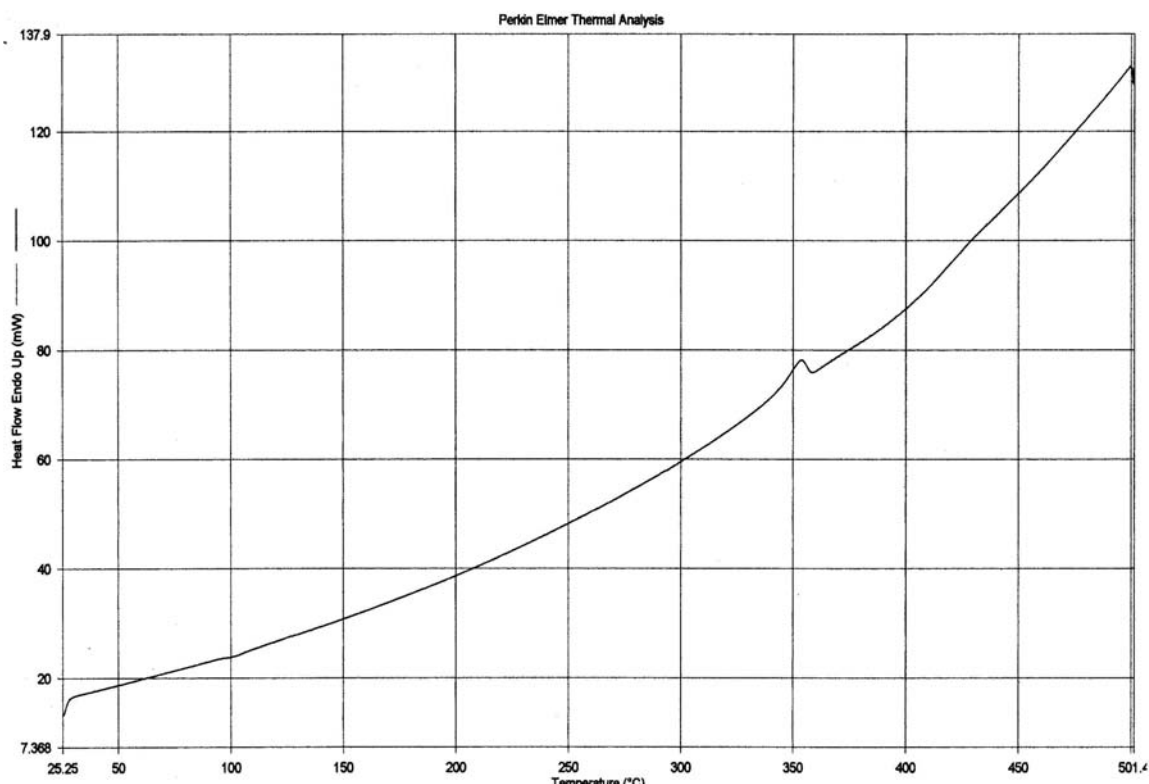


**Figure 26.** DSC plot of TAMU-P3-1 from 23°C to 500°C at a rate of 20°C per minute.

There was no baseline applied to the DSC plot of TAMU-P3-1. It was not necessary to apply a baseline. The purpose of this DSC plot was to ascertain a crosslinking temperature range that could be used in the Fourier Transform Infrared Spectroscopy degree of cure test. The lack of a baseline gives the plot a different appearance to the DSC plot of AFR-PEPA-2. Several observations can be made. What is strikingly different from this DSC plot relative to the DSC plot from AFR-PEPA-2 (shown in Chapter III, Section 1), there is no  $T_g$  or melting of oligomer crystals found in the TAMU-P3-1 DSC plots. This change warrants that the TAMU-P3 may not contain any crystals. Also it has been found that the PMDA used in the new oligomer does not

have a  $T_g$  or  $T_m$  point. That is, these points are too high to be found by the typical thermal analysis methods. The material will degrade, before any point is discovered.

#### 4.3.2 Fourier Transform Infrared (FTIR) Spectroscopy and Degree of Cure Results

A FTIR spectrum was taken of the TAMU-P3-1 oligomer in its initial state, shown in Figure 27. There was significant evidence shown in the spectrum that the synthesis had been successful. There were several imide peaks that showed the specific bonding, especially Imide III, where the C-N bonds occurs. The presence of this bond shows that there was a successful linkage and imidization between the PMDA and *p*-PDA monomers.

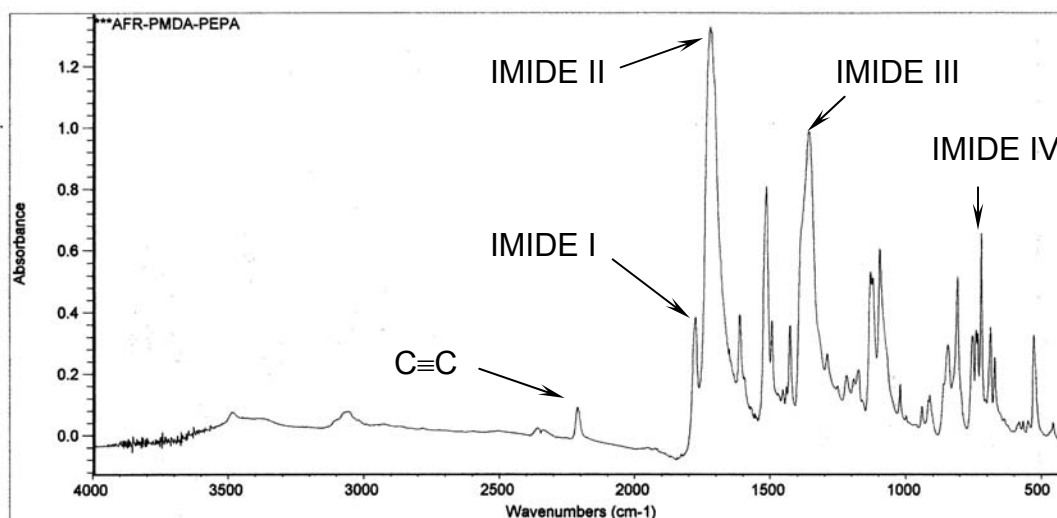


**Figure 27.** FTIR plot of TAMU-P3-1, uncured, showing significant imides and carbon-triple bond peak intensities.

Since the DSC plot showed a crosslinking peak at 351°C, the foot of the curve began around 340°C. The FTIR tests were employed at 340°C. The cure was chosen to be at four different lengths of time: 5 minutes, 15 minutes, 30 minutes, and one hour. The degree of cure is determined using the equation below:

$$\alpha = (I_{C\equiv C} / I_n)_t / (I_{C\equiv C} / I_n)_{t=0} [3] \quad (1)$$

where  $\alpha$  is the degree of cure,  $I$  is the peak intensity of either the carbon triple bond or the normalizing peak,  $n$  is the peak used to normalize the results, and  $t$  is the given length of time the specimen was cured. The peaks used in the calculations are explained in Table 5. The table explains what type of bonding exists at the displayed frequencies. The carbon-triple bond occurs around 2210 (1/cm). Over time, as the material cures, the carbon-triple bond is consumed. The degree of cure is plotted with respect to time and normalization peaks.



*Table 5. Peak assignments to normalize the intensity of the crosslink reaction.*

<b>Peak Assignment</b>	<b>Wavenumber (1/cm)</b>	<b>Description of Imide</b>
Imide I	1777	C=O Asymmetrical Stretching
Imide II	1724	C=O Symmetrical Stretching / Aromatic Imide
Imide III	1360	C-N Stretching / Aromatic Imide
Imide IV	741	C=O Bending / Aromatic Imide
Crosslinking Reaction	2210	Carbon triple bond Absorption

As in AFR-PEPA-N, the carbon triple bond peak at 2210 1/cm slowly decreased in intensity as the cure time increased. Another interesting peak arose at 2359.58 and 2340.52 1/cm. These two grouped peaks decreased as the cure time increased. The interesting subject to note here is that these peaks did not exist in the original FTIR scans prior to the curing of the test specimens. This could be that there is additional bonding occurring and decreases at the cure time increases. Another possibility is that the chemistry of the compressed disks changed over the period of time of when it was produced and when it was cured. A week-long period had passed before these specimens were cured. The amount of cure changes with respect to imide peak intensity that was used to normalize the data.

In Figure 28, the initial degree of cure is varies greatly between the different normalization imides used. But the degree of cure levels off between 80 to 90 percent cure. The Imide 2 curve warrants the most conservative degree of cure, only reaching 80% degree of cure at 60 minutes. If given more time, the degree of cure could possibly

slightly increase, however in Lincoln's study AFR-PEPA-N only reached approximately 50 to 60 percent degree of cure. Lincoln's experiment does differ in specimen preparation and may not be a suitable comparison.

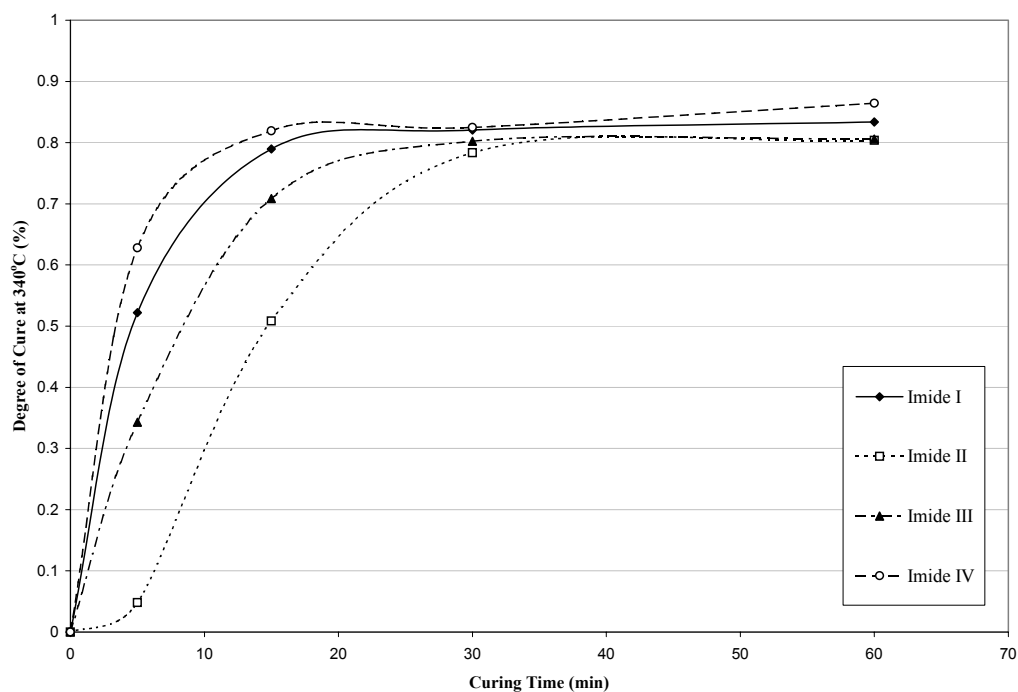


**Figure 28.** Degree of cure of TAMU-P3-1 at 340°C over time, comparing normalizing imides.

#### 4.3.3 Dissolution and Liquid-Crystalline Test

The 0.01 gm of TAMU-P3-1 and 10 ml of NMP were blended together at room temperature for a 24 hour period. The TAMU-P3 did not completely dissolve in the NMP solvent solution. Powder crystals remained at the bottom of the solution. The

solution should be dissolved at an elevated temperature to find at what point the oligomer will dissolve.

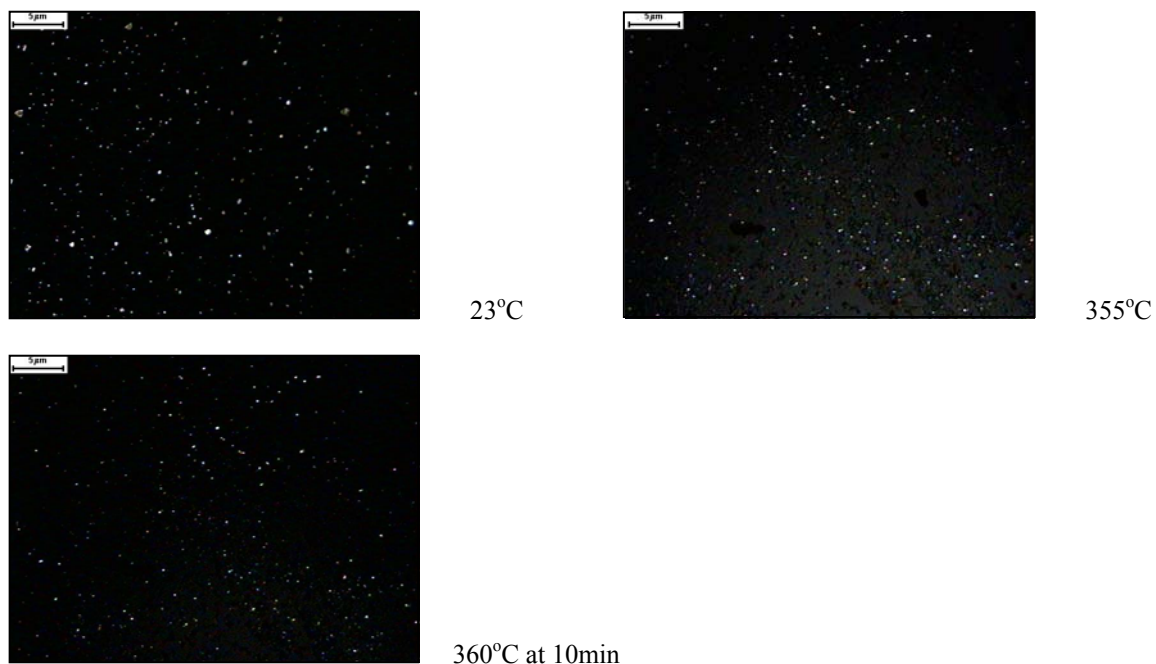


**Figure 29.** Pictographs of undissolved TAMU-P3-1 imide oligomer crystals and heated to 360°C and held at 360°C for 10 minutes (seen in real time).

There was no image change within the film as it was being heated over time as seen in Figure 29. No special artifacts arose during the heating. No crystal melted as well. Based on other liquid-crystalline studies, there were no liquid-crystalline behavior noticed as the film was heated and viewed in real time.

#### 4.4 Conclusions

- ◆ The remodification of AFR-PEPA-N was completed by substituting the fluorinated backbone with a more rigid rod-like monomer. The synthesis of this new polyimide oligomer deemed successful in the following initial characterization studies.
  
- ◆ Initial characterization of TAMU-P3 showed that the oligomer cures at a temperature of 350°C from DSC findings. The degree of cure reaches about 80 to 90 percent complete based upon the consumption of the carbon-triple bond.
  
- ◆ TAMU-P3 has difficulties in completely dissolving within NMP. This could lead to problems in processing this oligomer, allowing defects within the cured structure.
  
- ◆ TAMU-P3 has not shown any signs of liquid-crystalline behavior due to the lack of typical signs of LC characteristics in pictures taken from film shown in cross-polarized light inconjunction with a heating stage.

## CHAPTER V

### CONCLUSIONS

#### 5.1 Conclusions

In this thesis, the precured and cured polyimide, AFR-PEPA-N oligomer's special characteristics were investigated for any possible (i) crystalline and (ii) liquid-crystalline characteristics using birefringence and other methods. A reasonable processing window was found due to the finding that the crystal size could be reduced by appropriate dissolution techniques. The residual oligomer crystals were found to be innate in the powder and not created by thermal processing.

The potential temperature overlap was found to be between 360°C and 375°C and the crystals could not melt entirely before the material began crosslinking. Possible nematic liquid-crystalline characteristics were found to be present at 360°C and that a new polyimide that originates from this structure could contain the high thermal, mechanical, degradation stability as well have the optimum properties due to its liquid-crystalline nature.

Chapter IV introduces a new polyimide based upon AFR-PEPA-N's original structure. The remodification of AFR-PEPA-N was completed by substituting the fluorinated backbone with a more rigid rod-like monomer.

Initial characterization of TAMU-P3 showed that the oligomer cures at a temperature of 350°C from DSC findings. The degree of cure reaches about 80 to 90 percent complete based upon the consumption of the carbon-triple bond. TAMU-P3 did not completely dissolve within NMP. If heat is applied to this solution TAMU-P3 could possibly dissolve completely. TAMU-P3 did not show signs of liquid-crystalline behavior that AFR-PEPA-N showed when held at a high isotherm.

## **5.2 Suggestions for Future Work**

To further develop the high temperature polyimide, which is, will have a higher possibility for liquid-crystalline behavior. One approach is to create rigid-rod imide oligomers that will self-align and assemble by developing oligomers that contain ionic ends. The hydrogen within the acetylene endgroups can be replaced with an ionic salt. The advantages of these self-assembling linear rods would create an anisotropic product with exceptional mechanical, optical and electrical properties. The oligomer rods could be oriented and when the polymer is cured, crosslinks will be created along the orientation axis of the crystals, resulting in networks with segments of equal load bearing characteristics.

## REFERENCES

1. Morgan, R. J., E. E. Shin, J. E. Lincoln, and Zhou J. (2001). Overview of polymer matrix composites performance and materials development for aerospace applications, *SAMPE Journal*, Mar-April, **37** (2):102-107.
2. Chang, K. C. and Waters J. E. (1995). Effects of endcaps on the properties of polyimide/carbon fiber composites. In: *Proc. of 40<sup>th</sup> International SAMPE Symposium*. Vol. 40. Anaheim, California, 8-11 May. pp. 1113-1136.
3. Lincoln, J. E. (2001). Structure-property-processing relationships and the effects of physical structure on the hygrothermal durability and mechanical response of polyimides, *An Abstract of a Dissertation Michigan State University: Dept. of Materials Science and Mechanics*.
4. Ghosh, M. K. and Mittal, K. L. (1996). *Polyimides: Fundamentals and Applications*. Marcel Dekker, Inc., New York.
5. Morgan, R. J. and O'Neal, J. E. (1977). The failure processes, morphology and mechanical properties of a co-polyimide glass based on benzophenone tetracarboxylic acid dianhydride. *Journal of Materials Science*, **12**: 1338-1348.
6. Morgan, R. J. (2001). Development and characterization of new, high performance polymers. *Texas Engineering Experiment Station*, Proposal # 000512 - 0190 – 2001.
7. Morgan, R. J. (2001). High temperature, organic, nanorod-based structures. *Texas Engineering Experiment Station [Internal Paper]*.
8. Wilson, D., Stenzenberger, H. D., and Hergenrother, P. M. (1990). *Polyimides*. Blackie & Sons Ltd., Glasgow.
9. Chung, T. -S. (2001). *Thermotropic Liquid Crystal Polymers: Thin-film Polymerization, Characterization, Blends, and Applications*. Technomic Publishing Co. Inc., Lancaster, PA.
10. Vainshtein, B. K., V. M. Fridkin, and Indenbom, V. L. (2000). *Modern Crystallography: Structure of Crystals*, Vol. 2, 3<sup>rd</sup> Edition. Springer, London.
11. Lincoln, J. E., R. J. Morgan, and Shin, E.E. (2001) Effect of thermal history on the deformation and failure of polyimides, *Journal of Polymer Science: Part B*, **39**: 2947-2959.

12. Dowell, F. (1989). Prediction and design of first super-strong mostly-rigid polymers from very molecular theories for smectic and nematic Polymers. *The Materials Science and Engineering of Rigid-Rod Polymers*, **134**: 33-46.
13. Lenhert, P.G. and Adams, W. W. (1989). X-Ray diffraction studies of the axial tensile modulus of rigid-rod polymers. *The Materials Science and Engineering of Rigid-Rod Polymers*, **134**: .329-340.
14. Wunderlich, B. and Chen, W. (1996). The difference between liquid crystals and conformationally disordered crystals. In: *Liquid-Crystalline Polymer Systems: Technological Advances*. ACS Series 632, American Chemical Society, 232-248.
15. Odell, J. A., A. Keller, E. D. T. Atkins, M. J. Nagy, J. L. Feijoo, and Ungar, G. (1989). Orientability of rigid rodlike molecules in solution and controlled preparation of model systems. *The Materials Science and Engineering of Rigid-Rod Polymers*, **134**: 223-234.
16. Rozenberg, B. A. and Gur'eva, L. L. (1996). Ordered liquid-crystalline thermosets. In: *Liquid-Crystalline Polymer Systems: Technological Advances*. ACS Series 632, American Chemical Society, 372-388.
17. Arnold, F. E. (1989). The birth of ordered polymer technology for air force applications. *The Materials Science and Engineering of Rigid-Rod Polymers*, **134**: 75-82.
18. Lusignea, R. W. (1989). Film processing and applications for rigid-rod polymers. *The Materials Science and Engineering of Rigid-Rod Polymers*, **134**: 265-276.
19. Denny, L. R., I. J. Goldfarb, and Soloski, E. J. (1989). Thermal stability of rigid-rod polymers. *The Materials Science and Engineering of Rigid-Rod Polymers*, **134**: 395-412.
20. Martin, D. C. and Thomas, E. L. (1989). Morphology of rigid-rod polymer fibers: An overview. *The Materials Science and Engineering of Rigid-Rod Polymers*, **134**: 415-429.
21. Baker, L. N., H. C. Knachel, A.V. Fratini, and Adams, W. W. (1989). Structural transformations in crystalline oligomers of polyparaphenylene. *The Materials Science and Engineering of Rigid-Rod Polymers*, **134**: 497-503.



22. Cheng, K.-Y and Lee, Y. -D. (1996). Molecular composites of liquid-crystalline polyamides and amorphous polyimides: Synthesis, rheological properties, and processing, In: *Liquid-Crystalline Polymer Systems: Technological Advances*. ACS Series 632, American Chemical Society, 22-38.
23. Kyu, T., J. -C yang, C. Shen, M. Mustafa, C. J. Lee, F. W. Harris, and Cheng, S. Z. D. (1996). Miscibility, structure, and property of poly(biphenyl dianhydride perfluoromethylbenzidine)-poly(ether imide) molecular composites. In: *Liquid-Crystalline Polymer Systems: Technological Advances*. ACS Series 632, American Chemical Society, 39-53.

## APPENDIX

Lincoln summarizes thermooxidation degradation mechanisms for polyimides in composite form at the macroscopic level as stated:

- (i) Oxidation begins at the surface of the polymer matrix, forming an oxidation layer that has a different chemical composition than the original matrix and can be seen in the microstructure. Weight loss occurs primarily in the surface layer.
- (ii) If the temperature is high enough chemical degradation or reaction by-products and volatiles will diffuse out of the resin.
- (iii) Over time, the surface layer increases and microcracks and voids begin to form at the surface. Voids increase in size, density, and act as points for microcracks to grow.
- (iv) Microcracks also form in the composite interior due to the mechanisms mentioned earlier. Cracks in the laminate enhance oxidation of the composite by providing additional paths for oxygen penetration, leading to a vicious circle, with oxidation promoting cracking, allowing more oxidation, and so on [3].

## VITA

Lindsay Adams Murphy was born in Norristown, Pennsylvania, on December 27, 1978. At age fourteen, she moved with her family to The Woodlands, Texas. She graduated Summa Cum Laude from The Woodlands High School in the spring of 1997. Lindsay went on to receive her Bachelors of Science degree in mechanical engineering from Texas A&M University in August 2001. That same year she began her graduate studies at Texas A&M University in mechanical engineering. In 2002, she received the Society of Plastics Engineers Scholarship for graduate students. In 2003, she was awarded a National Science Foundation grant to work with other researchers at Pohang University of Science and Technology (POSTECH), Pohang, South Korea for an eight-week period.

Her permanent address is:

82 Amberglow Ct.

The Woodlands, TX 77381

Her e-mail address is:

Pepino\_01@yahoo.com